PHILOSOPHICAL TRANSACTIONS OF THE ROYAL SOCIETY A MATHEMATICAL, PHYSICAL & ENGINEERING SCIENCES

Geochemical arguments for an Earth-like Moon-forming impactor

Nicolas Dauphas, Christoph Burkhardt, Paul H. Warren and Teng Fang-Zhen

Phil. Trans. R. Soc. A 2014 **372**, 20130244, published 11 August 2014

PHILOSOPHICAL TRANSACTIONS OF THE ROYAL SOCIETY A

rsta.royalsocietypublishing.org

Research

Cite this article: Dauphas N, Burkhardt C, Warren PH, Teng F-Z. 2014 Geochemical arguments for an Earth-like Moon-forming impactor. *Phil. Trans. R. Soc. A* **372**: 20130244. http://dx.doi.org/10.1098/rsta.2013.0244

One contribution of 19 to a Discussion Meeting Issue 'Origin of the Moon'.

Subject Areas:
geochemistry, solar system

Keywords:
Moon, isotopes, impact, origin

Author for correspondence:
Nicolas Dauphas
e-mail: dauphas@uchicago.edu

Electronic supplementary material is available at http://dx.doi.org/10.1098/rsta.2013.0244 or via http://rsta.royalsocietypublishing.org.

Royal Society Publishing

Geochemical arguments for an Earth-like Moon-forming impactor

Nicolas Dauphas[1], Christoph Burkhardt[1], Paul H. Warren[2] and Fang-Zhen Teng[3]

[1]Origins Laboratory, Department of the Geophysical Sciences and Enrico Fermi Institute, University of Chicago, 5734 South Ellis Avenue, Chicago, IL 60637, USA
[2]Institute of Geophysics and Planetary Physics, University of California, Los Angeles, CA 90095-1567, USA
[3]Isotope Laboratory, Department of Earth and Space Sciences, University of Washington, Seattle, WA 98195, USA

Geochemical evidence suggests that the material accreted by the Earth did not change in nature during Earth's accretion, presumably because the inner protoplanetary disc had uniform isotopic composition similar to enstatite chondrites, aubrites and ungrouped achondrite NWA 5363/5400. Enstatite meteorites and the Earth were derived from the same nebular reservoir but diverged in their chemical evolutions, so no chondrite sample in meteorite collections is representative of the Earth's building blocks. The similarity in isotopic composition (Δ^{17}O, ε^{50}Ti and ε^{54}Cr) between lunar and terrestrial rocks is explained by the fact that the Moon-forming impactor came from the same region of the disc as other Earth-forming embryos, and therefore was similar in isotopic composition to the Earth. The heavy δ^{30}Si values of the silicate Earth and the Moon relative to known chondrites may be due to fractionation in the solar nebula/protoplanetary disc rather than partitioning of silicon in Earth's core. An inversion method is presented to calculate the Hf/W ratios and ε^{182}W values of the proto-Earth and impactor mantles for a given Moon-forming impact scenario. The similarity in tungsten isotopic composition between lunar and terrestrial rocks is a coincidence that can be explained in a canonical giant impact scenario if an early formed embryo (two-stage model age of 10–20 Myr) collided with the proto-Earth formed over a more protracted accretion history (two-stage model age of 30–40 Myr).

1. Introduction

The Earth formed by collisions with Moon to Mars-size planetary embryos [1–3]. One such collision probably led to the formation of the Moon [4–9]. Several key observables are available to constrain scenarios of the formation of the Moon, including the angular momentum of the Earth–Moon system, the lunar core size and the geochemistry of the Moon. Recently, high-precision measurements of lunar rocks have revealed a high degree of isotopic similarity between lunar and terrestrial rocks for elements that display nucleosynthetic anomalies (^{17}O, ^{50}Ti and ^{54}Cr) [10–17], radiogenic ingrowth due to core partitioning (^{182}Hf–^{182}W, $t_{1/2} = 9$ Myr) [18–20], and stable isotopic fractionation possibly due to metal–silicate segregation (Si) [21–23]. Hydrocode modelling of the formation of the Moon [24] predicts that most (approx. three-quarters) of the lunar material should be derived from the impactor, the rest being contributed by the proto-Earth mantle [9,25]. If the impactor had a different isotopic composition from the Earth, which some have argued is likely [26], the composition of lunar samples should differ from terrestrial samples. Instead, the Moon is isotopically very similar to the Earth, questioning existing models of the Moon formation. This lunar isotopic crisis has motivated new versions of the giant impact theory such as isotopic equilibration between the proto-Earth mantle and the protolunar disc mediated by gas in the aftermath of the giant impact [26], formation of the Moon from the Earth by impact of a small embryo with a fast-spinning Earth and subsequent despinning through resonances [7], or collision between two equal-size bodies [8]. These new scenarios can potentially resolve some of the isotopic problems of the Moon-forming impact, but this is at the expense of simplicity, as new ad hoc hypotheses are made. In this contribution, we evaluate all geochemical evidence bearing on the nature of the Moon-forming impactor and conclude that the Earth accreted from embryos with very uniform isotopic compositions (similar to enstatite chondrites, aubrites and ungrouped achondrite NWA 5363/5400), so most likely the Moon-forming impactor had an isotopic composition very similar to the proto-Earth.

2. Nuclear isotope anomalies

Isotope variations can arise due to nuclear transmutations (radiogenic, nucleogenic and cosmogenic production), stable isotope fractionation (kinetic or equilibrium) and stellar nucleosynthesis. In this section, we focus on isotope variations that are present at the scale of bulk planetary bodies and depart from the laws of mass-dependent fractionation. These planetary scale isotope anomalies are extremely useful to identify relationships between planetary bodies. Indeed, most nebular, disc and planetary processes that can affect stable isotope ratios usually follow the law of mass-dependent fractionation, which does not affect isotope anomalies that are defined as departures from mass-dependent fractionation. This means that isotope anomalies can see through mass-dependent secondary processes, to establish relationships between planets and meteorites.

Oxygen was the first element for which planetary scale isotope anomalies were observed [27]. The origin of these anomalies is still uncertain but could have involved CO photochemistry in the inner disc [28], in the outskirts of the Solar System [29] or in the interstellar medium [30]. More recently, planetary scale isotopic anomalies have been discovered for elements with various geochemical affinities, in particular for molybdenum [31–34], ruthenium [35–37], calcium [38,39], titanium [14,40], chromium [15,41,42], nickel [43–45], tungsten [46], strontium [47,48], barium [47,49,50], samarium and neodymium [50,51]. Discussing the origin of these anomalies is beyond the scope of this paper. It is sufficient to know that they reflect a heterogeneous distribution of presolar grains that carry nucleosynthetic anomalies inherited from the stellar outflows where those grains condensed [31,52,53].

Isotopic anomalies have been at the centre of much attention in the context of Moon-forming scenarios, as they can potentially provide constraints on the fraction of the Moon that is derived from the proto-Earth mantle and the impactor. Meteorite samples show large isotope heterogeneity between meteorite groups. If this heterogeneity is representative of the variations

in isotopic compositions of the embryos that impacted the Earth, then there is no reason why the Moon-forming impactor should have had the same isotopic composition as the proto-Earth. Given that in the canonical model the Moon is made of approximately one-fourth proto-Earth and approximately three-fourths impactor [9,25], one would expect to find measurable isotopic differences between lunar and terrestrial rocks [26]. However, no or little difference has been detected so far for all elements that have been analysed at high precision, namely oxygen [10–13,17], chromium [15,16] and titanium [14].

Most studies have found indistinguishable $\Delta^{17}O$ (deviation of the $^{17}O/^{16}O$ ratio from the terrestrial fractionation line in permil) between lunar and terrestrial rocks (within approx. 0.02‰ compared to approx. 7‰ variation among meteorites [10–13]), while Herwatz *et al.* [17] recently reported the finding of a small difference in $\Delta^{17}O$ of only $+0.012 \pm 0.006$‰. Pahlevan & Stevenson [26] argued that the protolunar disc and Earth's mantle started with more contrasted oxygen isotopic compositions, but that the difference was erased by isotopic exchange between the silicate Earth and the protolunar disc in the aftermath of the giant impact. Such gas-mediated equilibration may be difficult to achieve for highly refractory elements like titanium, yet the $\varepsilon^{50}Ti$ (deviation in parts per 10 000 of the $^{50}Ti/^{47}Ti$ ratio from a terrestrial standard after correction for mass-dependent fractionation by internal normalization) values of lunar and terrestrial rocks are indistinguishable within $\pm 0.04\,\varepsilon$-units compared to 6 ε-units variation among meteorites [14]. A second difficulty of the equilibration scenario is that it predicts $\delta^{30}Si$ isotopic fractionation of approximately 0.14‰ in the Moon relative to the Earth's mantle [54], which is not found [21–23]. More recently, two impact models that invoke impact of a small embryo with a fast-spinning Earth [7] or impact between two equal-size bodies [8] have been proposed to explain the isotope similarities between lunar and terrestrial rocks. Both models predict a higher angular momentum in the Earth–Moon system than is observed, but some of that excess could have been dissipated through an orbital resonance between the Sun and the Moon [7].

The lunar isotopic crisis arises from the notion that the embryos that formed the Earth had variable isotopic compositions and in particular that the Moon-forming impactor displayed isotopic anomalies relative to the proto-Earth [26]. We review below the geochemical arguments pertaining to this issue and conclude that most likely, the Earth was accreted from a population of embryos with uniform isotopic compositions and that the Moon-forming impactor thus also had an isotopic composition similar to the proto-Earth.

The first argument stems from the remarkable similarity between terrestrial rocks and EH, EL chondrites, aubrites and a new ungrouped achondrite NWA 5363/5400 (see [39] for further discussions). Pahlevan & Stevenson [26] speculated that the embryos that formed the Earth had variable isotopic compositions, because they formed in a disc that showed a gradient in oxygen isotopic composition. During oligarchic growth, embryos are accreted from material from a relatively narrow annulus (5–10 Hill radii) [55], so the disc heterogeneity is directly mapped onto embryos. In this scenario, the similarity between the oxygen isotopic composition of the Earth on the one hand, and EH, EL chondrites, aubrites and NWA 5363/5400 on the other hand, is a mere coincidence, reflecting the contributions of various embryos that average to the oxygen isotopic composition of some particular meteorite groups. However, several elements other than oxygen (calcium, titanium, chromium, nickel and molybdenum) display isotopic anomalies at a bulk planetary scale [14,15,31–34,38–45] (figure 1). One can ask the question of what is the likeliness that a fully grown planet matches exactly the isotopic composition of a few meteorite groups that represent a snapshot in time of dust in the protoplanetary disc? What is the chance that the Earth's isotopic composition closely matches that of a hand specimen of enstatite chondrites made of chondrules and matrix and weighing 10^{24} times less? Various processes (e.g. photochemistry, nuclear statistical quasi-equilibrium, p-, r- and s-processes) produced isotopic anomalies on ^{17}O, ^{54}Cr, ^{50}Ti, ^{48}Ca, ^{62}Ni and ^{92}Mo, which as a result are not all correlated. It would therefore take extraordinary circumstances for random collisions between isotopically disparate embryos to match that of EH, EL chondrites, aubrites and possibly NWA 5363/5400 (only $\Delta^{17}O$ and $\varepsilon^{54}Cr$ have been measured in this sample [57]).

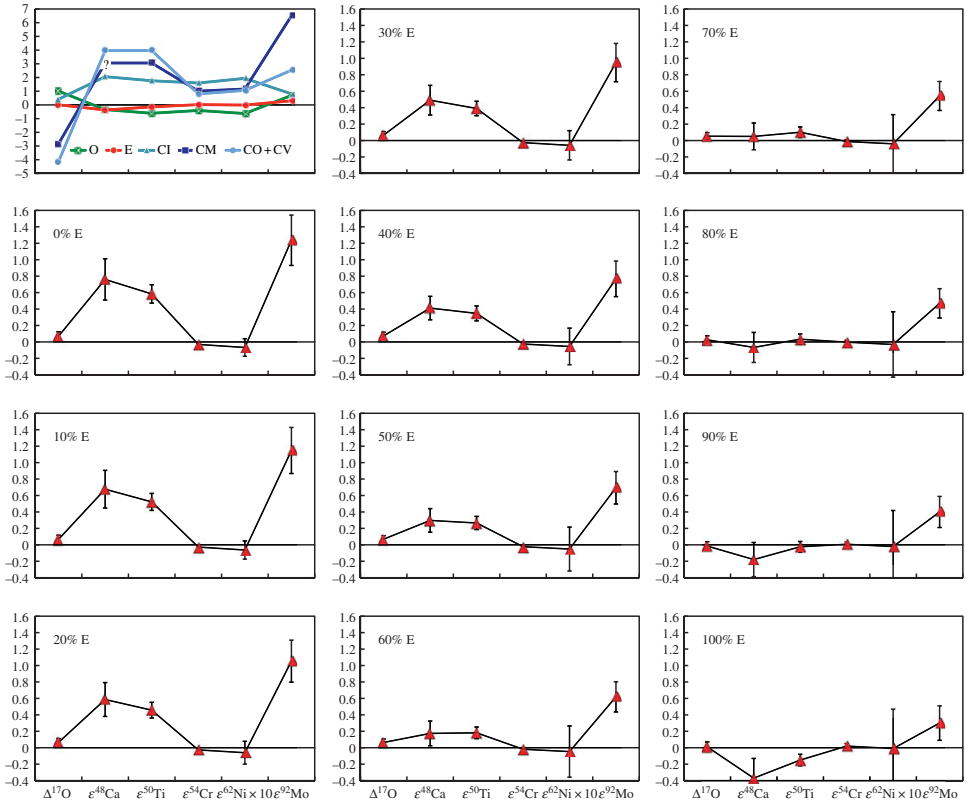

Figure 1. Constraints from isotopic anomalies (Δ^{17}O, ε^{48}Ca, ε^{50}Ti, ε^{54}Cr, ε^{62}Ni and ε^{92}Mo) on the building blocks of the Earth [39]. The top left panel shows the isotopic anomalies in bulk chondrites (see [39] and references therein for values). Because ordinary chondrites (H, L and LL), enstatite chondrites (EH and EL) and CO, CV carbonaceous chondrites have isotopic compositions that are very close, they are lumped together in the O, E and CO + CV supergroups. Because ε^{48}Ca–ε^{50}Ti and ε^{54}Cr–ε^{62}Ni tend to correlate [56], these isotope pairs do not provide independent constraints on the building blocks on the Earth but the remaining isotopes are sufficient to decompose mixtures of five constituents (O, E, CI, CM and CO + CV). Here E refers to a nebular reservoir that has the same isotopic composition as enstatite chondrites but can have different chemistry (e.g. as exemplified by ungrouped achondrite NWA 5363/5400). For each panel, the fraction of E is fixed (from 0 to 100% in intervals of 10%) and the proportions of O, CI, CM and CO + CV isotopic reservoirs are changed to minimize the χ^2-value. No chondrite mixture can reproduce the isotopic composition of the Earth if E does not represent 70–100% of the mass of the Earth. Allowing the fraction of E to vary, the χ^2 is minimized for O = 6.8%, E = 90.8%, CI = 0.2%, CM = 0% and CO + CV = 2.3%. For approximately 90 ± 10% E, all isotopic anomalies of the Earth are reproduced except ^{92}Mo but this excess arises entirely from a single high-precision measurement of ε^{92}Mo in Abee [34] dominating the weighted average value of enstatite chondrites, which otherwise display no resolvable isotopic anomalies for molybdenum [32,34]. (Online version in colour.)

The only way around this is to consider instead that the Earth was accreted of material of constant isotopic composition, similar to enstatite meteorites [39] (figure 1). Enstatite chondrites have been considered as building blocks of the Earth [58–60], but their δ^{30}Si values and Mg/Si ratios are inconsistent with those measured in the Earth, which makes this hypothesis unlikely [22,23,61]. However, the similarity in isotopic compositions does not mean that the Earth was accreted from enstatite chondrites, but rather that they formed from the same isotopic reservoir and diverged in their chemical evolutions. The recently discovered ungrouped achondrite (brachinite-like) NWA 5363/5400 has a mineralogy and chemical composition distinct from enstatite chondrites and aubrites (e.g. it is dominantly Fo70 olivine, whereas enstatite chondrites are virtually devoid of FeO) but has oxygen and chromium isotopic compositions that are

indistinguishable from enstatite chondrites, aubrites and Earth [57]. Further work will be needed to characterize the isotopic composition of this sample, but it shows that the identity in isotopic composition does not imply identity in chemistry.

Herwartz *et al.* [17] recently reported the finding of a small difference of $+0.012 \pm 0.006‰$ in $\Delta^{17}O$ between lunar and terrestrial igneous rocks that they interpreted as evidence that the Moon-forming impactor was similar to enstatite chondrites, which are characterized by a $\Delta^{17}O$ value of $+0.050 \pm 0.012$ relative to the Earth. The conclusion of that study agrees with the case made here that the similarity in isotopic composition between the Earth and enstatite chondrites cannot be a coincidence but must reflect the fact that most Earth-forming embryos were similar isotopically to enstatite chondrites. The view that the Earth was accreted from isotopically disparate embryos [26] is only valid if the disc presented a large gradient in isotopic composition. Dauphas *et al.* [39] proposed instead that the inner disc was characterized by a uniform isotopic composition as far as 1.5 AU (IDUR for inner disc uniform reservoir). *The embryo that impacted the Earth to form the Moon was probably sourced from the same isotopically uniform reservoir that supplied Earth-forming embryos, which naturally explains the similarity in isotopic composition between the silicate Earth and the Moon*.

Even if the protoplanetary disc had uniform isotopic composition to 1.5 AU, 5–20% of the material that made Earth could have come from beyond 1.5 AU [62]. Note that other simulations predict a larger fraction originating from 1.5 AU (e.g. one-third in [63]) but the cut-off at 1.5 AU is arbitrary in the sense that its value is adjusted so that most of the Earth's building blocks came from that region (i.e. 1.5 AU in the simulations of [62]). The 5–20% of embryos originating from beyond 1.5 AU could have delivered water and volatile elements to the growing Earth [64] and their contributions could explain why, at very high precision, enstatite chondrites are shifted relative to terrestrial rocks in O [17], Ti [14] and possibly Mo [34] (however, see [32]) isotopic compositions.

A second geochemical argument for a Moon-forming impactor similar to the Earth as far as isotopic anomalies are concerned comes from examination of the molybdenum–ruthenium 'cosmic' correlation [33–37] (figure 2). Molybdenum and ruthenium display isotopic anomalies in bulk planetary objects that are due to variations in the contribution of matter from s-process nucleosynthesis. Both elements are present in chondrites and iron meteorites, allowing one to examine the degree of isotopic heterogeneity in parent bodies that are not accessible by measuring oxygen isotopes alone. Molybdenum and ruthenium display strongly correlated anomalies in all meteorite groups measured so far; $\varepsilon^{92}Mo = (-0.55 \pm 0.08) \times \varepsilon^{100}Ru + (0.08 \pm 0.18)$ (figure 2). Molybdenum is a moderately siderophile element, and one can show that most of its mantle inventory was delivered to the Earth before core formation [33]. Ruthenium on the other hand is strongly siderophile, so that it was completely scavenged into the core during Earth's accretion and all ruthenium now present in the mantle was added by a late veneer representing approximately 0.1–0.5% of Earth's mass that accreted after core formation [65–67].

Because molybdenum and ruthenium present in the Earth's mantle were delivered at different times of Earth's accretion (before and after the completion of core formation, respectively), one can use their isotopic compositions to evaluate the nature of the material that was accreted by the Earth at these two different stages [33,36,37]. The molybdenum isotopic composition of the bulk silicate Earth (BSE) is very close to enstatite chondrites, which is consistent with the picture given by lithophile element isotope anomalies (i.e. O, Ca, Ti and Cr) that only enstatite chondrites match approximately the isotopic composition of the Earth. If the material accreted as late veneer was different, then the isotopic composition of ruthenium in the BSE should reflect that. For example, if the late veneer was made of CM chondrites, as was proposed recently based on S–Se–Te abundance ratios [68] (however, see [69,70]), then $\varepsilon^{100}Ru$ would have been approximately -3.5 and the BSE would plot off the meteoritic $\varepsilon^{92}Mo$–$\varepsilon^{100}Ru$ correlation (i.e. at $\varepsilon^{92}Mo \approx 0$ and $\varepsilon^{100}Ru \approx -3.5$), which is not the case (figure 2). *The fact that the BSE plots on the ε^{92} Mo–ε^{100}Ru correlation defined by meteorites is consistent with the view that the isotopic composition of the material accreted by the Earth did not change before and after core formation and that this material came from the*

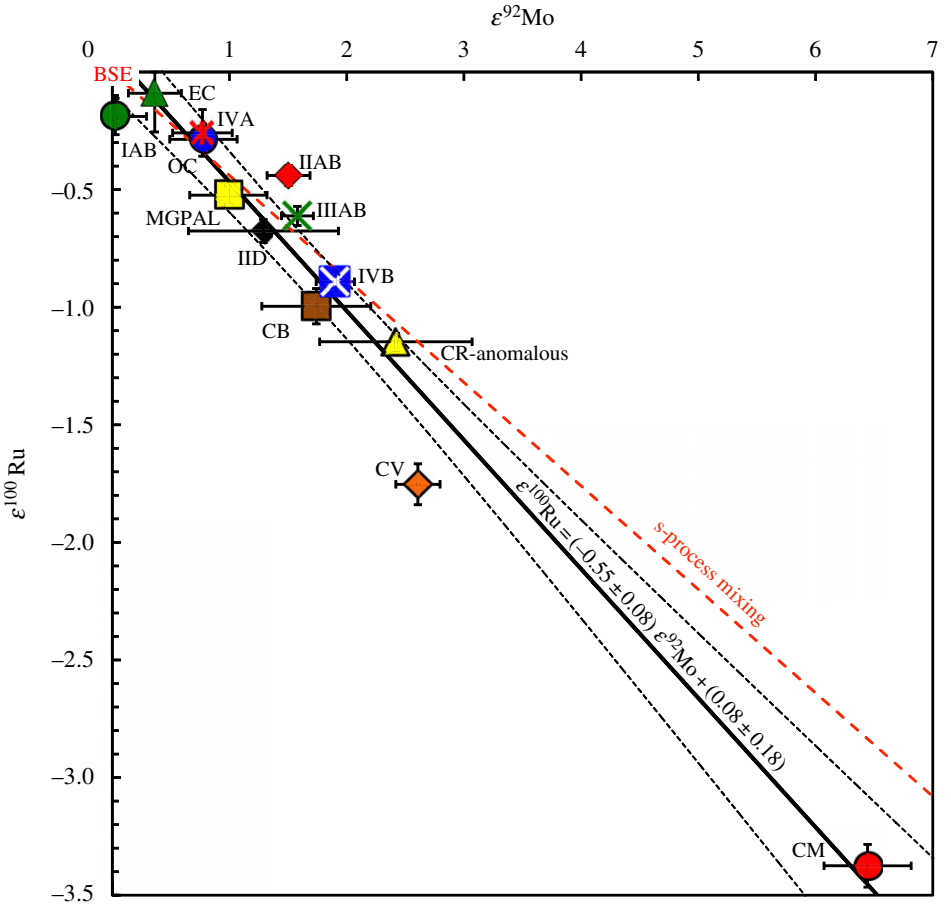

Figure 2. 'Cosmic' correlation between ε^{92}Mo and ε^{100}Ru among bulk meteorites (adapted from [33,34,36,37]). ε^{92}Mo values are from [31,32,34]. ε^{100}Ru values are from [35–37]. All specimens of a meteorite group have identical ε^{92}Mo and ε^{100}Ru, so only the group averages are plotted here. The dashed red line represents mixing between terrestrial and pure s-process composition (eqn (4) of [33]). The black dashed lines are the best-fit line and 95% confidence interval. Terrestrial standards are used for normalization of ε^{92}Mo and ε^{100}Ru values, so by definition, the BSE is exactly at the origin in this diagram. Molybdenum is a moderately siderophile element and mass-balance indicates that it was delivered to the Earth's mantle mostly during the main stage of Earth's accretion (i.e. relatively late but before the completion of core formation). Ruthenium on the other hand is highly siderophile, so that it was totally scavenged by core formation and Earth's mantle ruthenium inventory was delivered entirely by the late veneer (i.e. after core formation). ε^{92}Mo and ε^{100}Ru in Earth's mantle therefore record different stages of Earth's accretion. The position of the BSE relative to the line defined by chondrites in this diagram provides a critical constraint on the nature of the material accreted by the Earth before and after core formation. Let us assume for example that Earth's late veneer was of different nature from the material that made the bulk of the Earth. For a CM-like late veneer and E-like main accretion, the ε^{92}Mo value of the BSE would be approximately 0 while its ε^{100}Ru would be approximately −3.5. The BSE would thus plot very far off the correlation defined by bulk meteorites, which is not observed. The only way to explain why the BSE plots exactly on the correlation is if the material accreted by the Earth before and after core formation did not change in nature and was isotopically similar to E chondrites. BSE, bulk silicate earth; OC, ordinary chondrites; EC, enstatite chondrites; IAB, IIAB, IID, IIIAB, IVA, IVB = iron meteorites; MGPAL, main-group pallasites; CB, CM, CR, CV = carbonaceous chondrites. (Online version in colour.)

same nebular reservoir that made enstatite meteorites. The Moon-forming impactor was probably sourced from this same region of the disc, explaining the similarity in isotopic composition between lunar and terrestrial rocks.

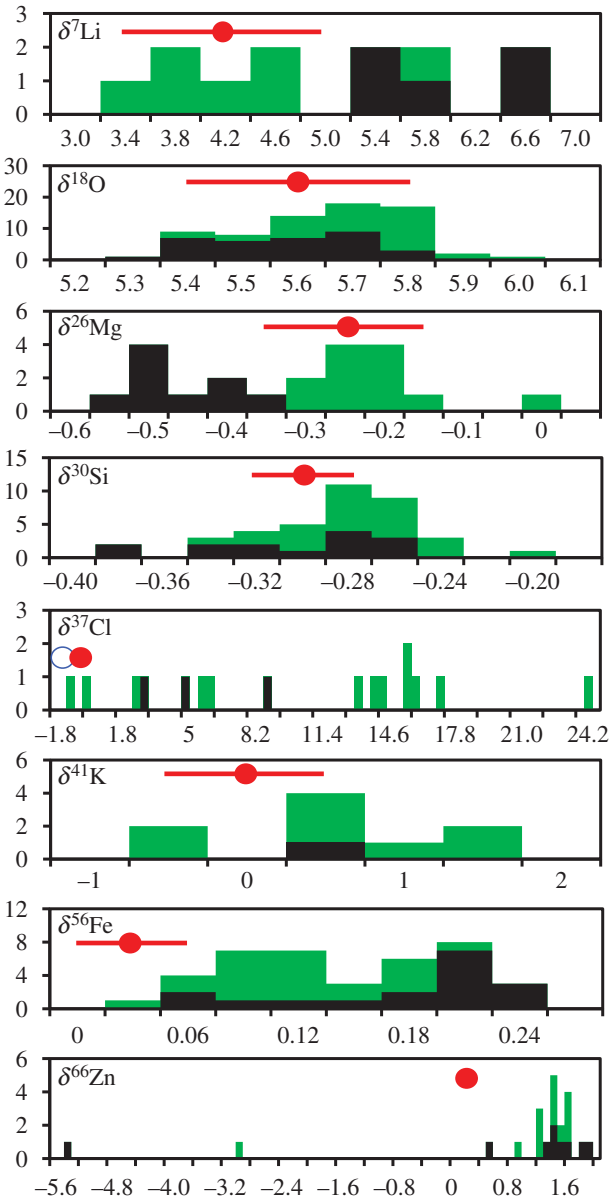

Figure 3. Histograms of Li [71,72], O [11–13,73], Mg [74], Si [21–23], Cl [75], K [76], Fe [73,77–79] and Zn [80] isotopic compositions of the Moon, as represented by lunar basalts (black, high-Ti basalts; green, low-Ti basalts) except for Cl, where samples include basalt, soil, regolith and apatite from basalts. The average isotopic compositions of the Earth (red dots) and typical uncertainties (horizontal red lines) for Li [81,82], O [83], Mg [84], Si [22,23,85–88], Cl [89,90], K [91], Fe [92,93] and Zn [80] are plotted for comparison. (Online version in colour.)

3. Silicon isotope systematics

High-precision isotopic analyses of lunar samples reveal different degrees of mass-dependent isotopic variations of volatile to moderately refractory elements Li [71,72], O [11–13,73], Mg [74], Si [21–23], Cl [75], K [76], Fe [73,77–79] and Zn [80] (figure 3). Magmatic processes such as lunar magma ocean crystallization, partial melting, magmatic differentiation and eruptive degassing can fractionate stable isotopes, so the isotopic composition of the Moon is uncertain for several

elements. For example, the heavy Fe isotopic composition of lunar basalts relative to the BSE has been ascribed to volatile loss during the giant impact [78] but lunar magma ocean differentiation and partial melting must be responsible for some of these variations [73,79]. Similarly, it was recently argued that the Moon has heavy zinc isotopic composition relative to the Earth due to volatile loss associated with the Moon-forming impact [80], but these variations could also be explained by $ZnCl_2$ volatilization during basalt eruption as has been suggested for chlorine [75]. Silicon is one of the few elements for which the lunar and terrestrial isotopic compositions are well known, providing important constraints on scenarios of Moon formation [21–23].

The first silicon isotope measurements suffered from interlaboratory biases [85,86,94,95] but more recent measurements are reproducible, and the discussion hereafter focuses mainly on the results from these studies. Silicon isotope measurements are reported using the δ^{30}Si notation, which is the deviation in parts permil of the $^{30}Si/^{28}Si$ ratio of the sample relative to the composition of the standard NBS-28: $\delta^{30}Si = [(^{30}Si/^{28}Si)_{sample}/(^{30}Si/^{28}Si)_{NBS\text{-}28} - 1] \times 10^4$. All studies of silicon isotope variations report measurements of geostandards BHVO-1 or BHVO-2 [21,23,61,85–88,96,97]. From these published data, we estimate that the interlaboratory reproducibility of δ^{30}Si measurements is approximately ±0.023‰, which we take to represent the accuracy at which silicon isotope compositions can be measured at present. A systematic error on δ^{30}Si of ±0.023‰ was therefore added quadratically to the statistical uncertainty of the mean δ^{30}Si value for each group of samples.

Georg *et al.* [94] first showed that the silicon isotope composition of the Earth was slightly heavier than that of chondrites. This work was followed by several studies that confirmed this observation and better constrained the silicon isotope composition of the silicate Earth and chondrites. Silicon isotopes can be fractionated during magmatic differentiation [88] but seem to be unaffected by partial melting (the most mafic magmas have silicon isotopic composition identical to mantle peridotites), so the BSE value can be calculated by taking the average value of primary mantle magmas (defined here as magmatic igneous rocks with $SiO_2 < 49$ wt%, $n = 20$) and mantle peridotites ($n = 33$), which yields a δ^{30}Si value of -0.297 ± 0.025 [23,61,85–88,96]. With an average δ^{30}Si value of -0.292 ± 0.026 ($n = 38$), lunar samples define a silicon isotopic composition for the Moon that is identical within uncertainties to that of the BSE [21,23,85] (figure 4). Chondrites have systematically lower δ^{30}Si values than the BSE, ranging from −0.7 to −0.45‰ [23,61,85,86].

The difference in silicon isotopic composition between the BSE and chondrites has been interpreted to reflect equilibrium stable isotopic fractionation between silicon in metal and silicate during core formation [23,85,86,94]. According to this picture, the bulk Earth would have a δ^{30}Si value similar to ordinary or carbonaceous chondrites and the heavy silicon isotopic composition of the BSE relative to chondrites would be balanced by a reservoir with a light silicon isotopic composition in the core. Theoretical and experimental studies support the view that partitioning between metal and silicate can fractionate silicon isotopes. Shahar *et al.* [100] estimated experimentally a metal–silicate equilibrium isotope fractionation for silicon that varies with temperature as $(-7.43 \pm 0.41) \times 10^6/T^2$ (T is in K), corresponding to a value of −0.8 at 3000 K. More recently, Hin *et al.* [101] obtained a fractionation factor that varies as $(-4.42 \pm 0.05) \times 10^6/T^2$, corresponding to a value of −0.5 at 3000 K. Hin *et al.* [98] suggested that the discrepancy with Shahar *et al.* [100] could be due to the fact that equilibrium was not completely reached in the latter study. Both sets of experiments agree qualitatively with molecular dynamics calculations that give a fractionation of approximately −0.6‰ at 3000 K [94,100]. Note that pressure seems to have little influence on equilibrium silicon isotopic fractionation between metal and silicate crystals [102] but the effect on melts is unknown.

Based on the isotopic fractionation between the BSE and chondrites for silicon, Georg *et al.* [94], Fitoussi *et al.* [85], Armytage *et al.* [86] and Zambardi *et al.* [23] concluded that a significant amount of silicon could be present in Earth's core (approx. 3–16 wt%, see table 2 of [23] for a compilation of published estimates) if the Earth was formed from material similar to known chondrites. These values correspond approximately to the amounts required to explain the density deficit of Earth's core [103].

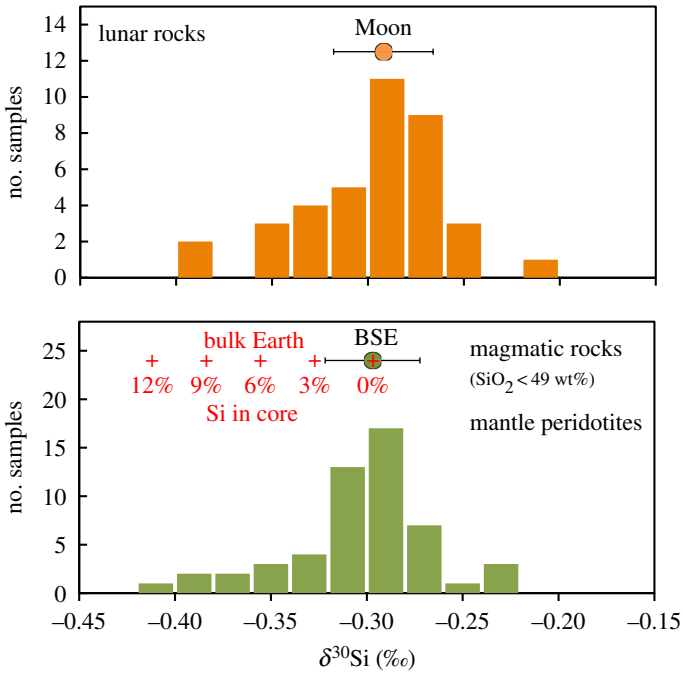

Figure 4. Histograms of the silicon isotopic compositions of lunar ($n = 38$) [21,23,85] and terrestrial samples (peridotites and magmatic rocks with $SiO_2 < 49$ wt%; $n = 53$) [23,61,85–88,96]. The data points are the best estimates of the silicon isotopic compositions of the Moon (-0.292 ± 0.026‰) and the BSE (-0.297 ± 0.025‰). The red crosses represent the estimated silicon isotopic composition of the bulk Earth for 0, 3, 6, 9 and 12 wt% Si in Earth's core (using the equilibrium fractionation factors of [98] at 3000 K). As shown, 3% or less of silicon in Earth's core [99] would induce little shift in the silicon isotopic composition of the BSE and no difference would be detectable between the BSE and the Moon if the Moon formed from three-fourths impactor (similar to the bulk Earth) and one-fourth proto-Earth mantle. (Online version in colour.)

The estimates based on silicon isotopes assume a bulk Earth silicon isotopic composition similar to ordinary or carbonaceous chondrites, although it is known that these meteorites do not match the isotopic composition of the Earth for most elements that display nuclear anomalies at a bulk planetary scale [56] (figure 1), a cardinal sin to be considered as building blocks for the Earth. Enstatite chondrites match the isotopic composition of the Earth for almost all elements but their low δ^{30}Si values (-0.69 ± 0.05‰ for EH, $n = 14$; -0.58 ± 0.03‰ for EL, $n = 10$) would require unrealistic amounts of silicon in Earth's core (more than 26 wt% [22,23,61]), far exceeding what is required to explain the core density deficit. An additional difficulty with an enstatite chondrite Earth is that the Mg/Si ratio of these meteorites is much lower than the BSE ratio, which would again take unrealistic amounts of silicon in Earth's core to balance. These difficulties led Fitoussi & Bourdon [22] to conclude that the Earth cannot be made of enstatite chondrites. The natural conclusion of these studies is that the Earth is not made of any chondrite material available in meteorite collections (also see [104,105]).

An important observation regarding silicon in the Earth is that the δ^{30}Si isotopic composition of chondrites correlates with the Mg/Si ratio (figure 5) [85]. The correlation is heavily leveraged by EH and EL, as ordinary and carbonaceous chondrites have similar δ^{30}Si values [61]. Nebular/disc processes must be responsible for these correlated variations and could have involved removal of high-temperature condensate forsterite from nebular gas [85], alloying of metal with silicon under reducing conditions [61] and sulfidation of silicates, a process that was invoked by Lehner *et al.* [109] to explain the low Mg/Si ratio of enstatite chondrites. An important constraint on the process responsible for fractionating Si isotopes and Mg/Si ratios is that it did not affect Mg isotopes, as the Mg isotopic composition of terrestrial rocks is chondritic [84,110–112]. Alloying of

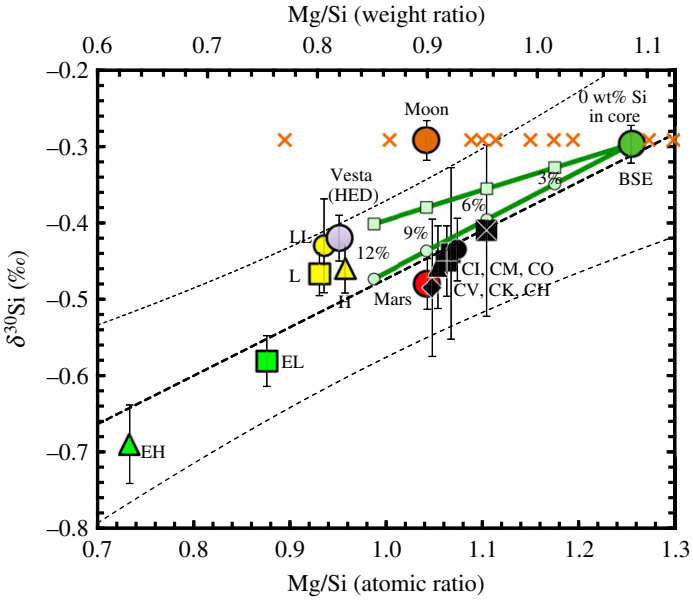

Figure 5. Relationship between silicon isotopic compositions (δ^{30}Si) and Mg/Si ratios (atomic ratio at bottom, weight ratio at top) of chondrites, Earth and Mars. The dashed lines are the regression of the chondrite data, $\delta^{30}\text{Si} = 0.63 \times (\text{Mg/Si})_{\text{atom}} - 1.11$, and the corresponding 95% prediction interval. The BSE Mg/Si atomic ratio (1.25) is from [106] and its δ^{30}Si (-0.297 ± 0.025) is the average of 53 measurements comprising 33 peridotites and 20 magmatic rocks with $SiO_2 < 49$ wt% [23,61,85–88,96]. The SiO_2 cut-off of 49 wt% was adopted because it corresponds approximately to the composition of primary mantle basalts and samples with higher SiO_2 contents may have experienced shallow-level differentiation. The two green lines give bulk Earth Mg/Si ratios and δ^{30}Si values for different amounts of Si in the core (0, 3, 6, 9 and 12 wt% [103]). The top line (light green squares) was calculated by assuming equilibrium metal–silicate δ^{30}Si isotopic fractionation at 3000 K of -0.5‰ [98] and the bottom line (light green circles) was calculated assuming a metal–silicate isotopic fractionation of -0.8‰ [100]. The Mg/Si atomic ratio of Mars (1.04) is from [107]. The δ^{30}Si value of Mars (-0.48 ± 0.03‰) is the average of 22 SNC measurements [23,86,97]. The Mg/Si of the Moon is from table 1 (the orange crosses are estimates from the literature; see figure 8). The δ^{30}Si of the Moon (-0.292 ± 0.026‰) is the average of 38 lunar rock measurements [21,23,85]. The Mg/Si ratio of Vesta is from [108]. The δ^{30}Si of Vesta (-0.42 ± 0.03) is the average of 12 howardite–eucrite–diogenite (HED) meteorites [97]. The chondrite data (Mg/Si atomic ratio; δ^{30}Si, number of δ^{30}Si measurements) are CI: (1.07; -0.44 ± 0.11, $n = 3$), CM: (1.05; -0.485 ± 0.090, $n = 4$), CO: (1.05; -0.458 ± 0.054, $n = 3$), CV: (1.07; -0.435 ± 0.041, $n = 12$), CK: (1.10; -0.41 ± 0.11, $n = 2$), CH: (1.06; -0.45 ± 0.05, $n = 1$), H: (0.96; -0.46 ± 0.03, $n = 7$), L: (0.93; -0.47 ± 0.03, $n = 8$), LL: (0.94; -0.43 ± 0.06, $n = 3$); EH: (0.73; -0.69 ± 0.05, $n = 14$) and EL: (0.88; -0.58 ± 0.03, $n = 10$). The references used in the chondrite compilation are [23,61,85,86]. (Online version in colour.)

Si in metal under reducing nebular conditions would not have affected Mg isotopes. Further work is needed to test the other two hypotheses but forsterite is rich in Mg and sulfidation increases Mg volatility, so variations in the isotopic composition of Mg may be expected. Whatever the process is, it could have affected the precursors of the Earth. In particular, the low Mg/Si ratios and δ^{30}Si values of enstatite chondrites relative to CI chondrites (representing solar composition) may have been balanced by higher Mg/Si ratios and δ^{30}Si values in other disc reservoirs. Thus, the only constraint for the bulk Earth composition is that it lies on the correlation defined by chondrites in the space δ^{30}Si versus Mg/Si.

A second important observation is that the BSE plots on the bulk chondrite δ^{30}Si versus Mg/Si correlation (figure 5). The BSE does not plot on a correlation δ^{30}Si versus Al/Si (e.g. fig. 2 of [61]) but part of the spread in Al/Mg ratio in carbonaceous chondrites must reflect the presence of calcium–aluminium-rich inclusions (CAIs) with high Al/Si ratios (CO, CV and CK contain 10–13 vol% CAIs). The fact that the BSE plots on the chondrite δ^{30}Si versus Mg/Si correlation means that the high values of δ^{30}Si and Mg/Si of the BSE relative to known chondrites may have

been inherited from material that is not sampled in meteorite collections. As shown in figure 5, the trajectory of nebular/disc fractionation is indistinguishable from that produced by silicon partitioning in the core, so at the present time, it is impossible to distinguish the two. Without understanding what caused δ^{30}Si and Mg/Si fractionation among chondrites and knowing what the Earth is made of, it is impossible to tell from δ^{30}Si values how much silicon is in the core.

The considerations above have important implications for the interpretation of the silicon isotope signature of the Moon. As discussed above, the δ^{30}Si value of the Moon (-0.292 ± 0.026) is indistinguishable from that of the BSE (-0.297 ± 0.025). Armytage *et al.* [21] argued that this implies that lunar silicon has equilibrated isotopically with the proto-Earth mantle. Owing to the small size and comparatively low pressure in the mantle of the Moon-forming impactor, silicon would not have partitioned into its core and its mantle should have chondritic silicon isotopic composition ($\delta^{30}\mathrm{Si}_{\mathrm{impactor}} \sim -0.45‰$) while the BSE silicon isotopic composition would have been fractionated by core formation ($\delta^{30}\mathrm{Si}_{\mathrm{BSE}} \sim -0.3‰$). If three-fourths of the Moon was derived from the impactor and one-fourth from the proto-Earth, the isotopic composition of the Moon should have been $3/4 \times \delta^{30}\mathrm{Si}_{\mathrm{impactor}} + 1/4 \times \delta^{30}\mathrm{Si}_{\mathrm{BSE}} = -0.41‰$, which is different from the BSE value. This is not observed, leading Armytage *et al.* [21] to conclude that lunar silicon saw core formation on the Earth, meaning that most of the Moon cannot be of impactor origin or that isotopic exchange occurred between the protolunar disc and the proto-Earth mantle. However, this calculation is entirely predicated on the assumption that the impactor and the bulk Earth have silicon isotopic compositions identical to ordinary and carbonaceous chondrites and that there is a significant amount of silicon in Earth's core.

As the BSE plots on the δ^{30}Si versus Mg/Si correlation defined by bulk chondrites, it is entirely possible that the Earth was made of material with δ^{30}Si and Mg/Si values similar to the BSE composition, with little silicon present in Earth's core (figure 5). For example, Badro *et al.* [99] argued that 2.8 wt% silicon and 5.3 wt% oxygen in Earth's core may be sufficient to explain geophysical constraints on sound velocities and density. Such a small amount would induce a small shift in the silicon isotopic composition of the BSE relative to the bulk Earth of approximately +0.03‰ [98]. If Earth's impactor had the same silicon isotopic composition as the bulk Earth and three-fourths of the Moon was derived from the impactor and one-fourth from the proto-Earth mantle, the difference in silicon isotopic composition between the Moon and the BSE would only be $0.03 \times 3/4 = 0.02‰$, which is not resolvable with current precision (figure 4). If the silicon concentration of the core is increased to 6 wt%, the calculated isotopic fractionation of the BSE relative to the bulk Earth becomes approximately +0.06‰ [98], which would produce a shift of 0.045‰ in the Moon using the same assumptions (one-fourth proto-Earth mantle + three-fourths impactor), which would be barely detectable (figure 4).

To summarize, the nature of the material that made the Earth is unknown and all evidence suggests that chondrites in collections are not representative of Earth's building blocks. Accounting for nebular/disc fractionation of δ^{30}Si and Mg/Si, it is conceivable that the Earth accreted from material with Si isotopic composition close to the present BSE composition, with no need to put large amounts of silicon in Earth's core (less than 6 wt% Si). A silicon concentration of approximately 3 wt% in Earth's core (together with approx. 5 wt% O) can account for observations of seismic velocities and density deficit in the core [99] but would lead to a shift in the silicon isotopic composition of Earth's mantle too small to be resolved with current analytical techniques (approx. +0.03‰ [98]; figure 4). *Therefore, the similarity in silicon isotopic composition between Earth's mantle and the Moon does not imply that the Moon formed from terrestrial material that saw high-pressure core partitioning of silicon. Instead, it may indicate that the Earth and Moon-forming impactor were made of the same precursor material that was fractionated by nebular and disc processes.*

4. Hf–W in the Earth–Moon–impactor system

The ^{182}Hf–^{182}W decay system ($t_{1/2} = 8.9$ Myr) is a versatile chronometer used to study the nature and time scales of planetary accretion, core formation and mantle differentiation [2,113,114]. Depending on the timing of core formation and the degree of Hf/W fractionation, the decay

of ^{182}Hf results in variable excess ^{182}W in the mantle relative to the bulk body. For large bodies, core formation is a protracted process and excess ^{182}W in their mantles depends on details of the accretion, such as the number and sizes of accreting planetary bodies, the degree to which metallic cores equilibrate with silicate mantles during collisions, and how strongly tungsten is subsequently partitioned into cores. As a result, calculated ages of core formation in terrestrial planets are, to some extent, model-dependent [113,115–117]. Nevertheless, the tungsten isotopic compositions of the Earth and the Moon can provide constraints on the formation of the Moon. In analogy to the nucleosynthetic anomalies discussed above, the impactor has left its tungsten isotope fingerprint in the Earth and Moon, which might be used to distinguish between different formation scenarios.

After correction of cosmogenic effects, Lee *et al.* [118] reported excess ^{182}W in lunar rocks of $+1.3 \pm 0.4\varepsilon$-units relative to Earth's mantle. Kleine *et al.* [119] subsequently measured lunar metals and found variable ^{182}W isotopic compositions ranging from approximately 0 to approximately $+2\varepsilon$-units relative to Earth's mantle. Touboul *et al.* [18] reported identical W isotope compositions between lunar and terrestrial mantles. More recently, Kleine *et al.* [19] found a small excess ^{182}W of $+0.17 \pm 0.08\varepsilon$-unit relative to terrestrial standards in lunar rocks characterized by low neutron-capture effects. The variable estimates illustrate the fact that the issue of the lunar tungsten isotopic composition may not be settled yet. Nevertheless, in the following we will take the most recent estimate at face value ($\varepsilon^{182}W_{\mathrm{Moon}} - \varepsilon^{182}\mathrm{W}_{\mathrm{BSE}} = +0.17 \pm 0.08$). The similarity in tungsten isotope composition between the Earth and Moon has been interpreted in three different ways: (i) the lunar and terrestrial mantles were equilibrated isotopically in the aftermath of the giant impact [26], (ii) the Moon is predominantly derived from proto-Earth material [14], a view that is at odds with canonical Moon-forming impact models suggesting that the Moon is mainly made of impactor material [6] but may be reconciled with more recent versions of the giant impact theory [7,8], and (iii) the mantles of the Moon-forming impactor and the proto-Earth had identical W isotope compositions, a scenario which is considered implausible because the impactor and the proto-Earth are thought to have followed different accretionary tracks [18,114].

Using the Hf/W ratios and the W isotopic compositions of the BSE and the Moon and under the premises of a canonical (i.e. approx. Mars-sized) impactor, we explore by mass-balance the Hf–W system parameter space for the impactor and the proto-Earth. Our mass-balance shows that the similarity in tungsten isotopic composition between lunar and terrestrial rocks can be well explained in the framework of a canonical collision between an early formed embryo and a proto-Earth that grew over a more protracted accretion history.

The two observable constraints of the Hf–W system, the Hf/W ratio and the W isotopic composition of a reservoir, are defined relative to the chondritic reference (CHUR, chondritic uniform reservoir) as

$$f = \frac{(\mathrm{Hf/W})_{\mathrm{reservoir}}}{(\mathrm{Hf/W})_{\mathrm{CHUR}} - 1} \tag{4.1}$$

and

$$\varepsilon\mathrm{W} = \left[\frac{(^{182}\mathrm{W}/^{183}\mathrm{W})_{\mathrm{reservoir}}}{(^{182}\mathrm{W}/^{183}\mathrm{W})_{\mathrm{CHUR}} - 1}\right] \times 10^4, \tag{4.2}$$

such that for a chondritic bulk planetary body at any time t after the start of the Solar System $f = \varepsilon\mathrm{W} = 0$. The terrestrial and lunar mantles have almost identical W isotope compositions ($\varepsilon\mathrm{W}_{\mathrm{Moon}} = +2.1 \pm 0.1$ [19] and $\varepsilon\mathrm{W}_{\mathrm{BSE}} = +1.9 \pm 0.1$ [117]) and Hf/W ratios ($f_{\mathrm{Moon,mantle}} = 25.7 \pm 3.3$ and $f_{\mathrm{BSE}} = 25.4 \pm 4.2$; based on re-evaluation of literature estimates [120–124] and using the chondritic Th/W and U/W ratios of [125]). In the electronic supplementary material, we demonstrate by mass-balance that for a given impact scenario mathematical relationships exist between the observables f_{BSE}, $\varepsilon W_{\mathrm{BSE}}$, f_{Moon}, $\varepsilon\mathrm{W}_{\mathrm{Moon}}$ and the compositions of the proto-Earth and impactor mantles $f_{\mathrm{impactor\ mantle}}$, $\varepsilon\mathrm{W}_{\mathrm{impactor\ mantle}}$, $f_{\mathrm{proto\text{-}Earth\ mantle}}$, $\varepsilon\mathrm{W}_{\mathrm{proto\text{-}Earth\ mantle}}$ (equations (23), (25), (39) and (41) of the electronic supplementary material). Solving the system of four equations returns the compositions of the proto-Earth and impactor mantles that reproduce

the compositions of the present-day terrestrial and lunar mantles. The uncertainties in the observables were propagated in the inversion by a Monte Carlo simulation (the dots in figure 6 represent 500 outcomes of these Monte Carlo simulations). Given the similar Hf/W ratios of the lunar and terrestrial mantles and assuming the Moon-forming impact occurred after the decay of ^{182}Hf (more than 50 Myr after the start of the Solar System [126]), we have omitted radiometric in-grow terms, such that today's εW values equal the ones at the time of the giant impact. We assume that the Moon-forming impact was the Earth's last major accretion event, followed only by accretion of a late veneer (0.3% of the mass of the Earth, 0.02% of the mass of the Moon [127]). We further assume that the impactor and proto-Earth have bulk chondritic compositions and that both bodies have silicate/metal (mantle/core) mass fractions identical to the present Earth, which seem plausible if they came from about the same heliocentric distance. Some objects in the Solar System, such as Mercury or the parent body of CB chondrites, contain significantly more metal than the Earth. However, given other sources of uncertainty, we have decided to restrict the parameter space investigated to impactors with Earth-like metal–silicate fractions. The Moon is made out of proto-Earth mantle, impactor mantle, impactor core and late veneer material. All simulations consider that the lunar core (approx. 2.5% of the mass of the Moon [128,129]) is made exclusively of impactor core material, which is suggested by all impact simulations [6,7,9,130] and is consistent with the near-terrestrial Fe/Mg ratio of the lunar mantle, which indicates that no iron reduction took place (see §5). The mass fraction of the Earth derived from the impactor is kept constant at 0.11 (Mars-sized impactor). Finally, k is the fraction of the impactor core re-equilibrating with the Earth mantle before being absorbed into Earth's core, i.e. $k = 1$ indicates full equilibration of the impactor core with the target mantle and $k = 0$ indicates no re-equilibration [131–133].

Our objective is to evaluate whether the W isotopic composition of the Earth–Moon system can be reconciled with a canonical scenario of lunar formation. The parameters used are therefore those relevant to such a collision and are summarized in table 1. The parameters that are the most poorly constrained and strongly influence the calculations (also see [132]) are the degree of equilibration between the impactor core and proto-Earth mantle (k), the metal–silicate partition coefficient for W during lunar core formation (D_M) and the fraction of the Moon that came from the impactor versus the proto-Earth mantle (h). For this reason, we present a range of simulations by varying k, D and h over acceptable ranges ($0 < k < 0.4$ [134,135]; $50 < D < 100$ [128,136]; $0.5 < h < 0.9$ [9,137]).

The results of the inversion calculations are presented in figure 6. An important conclusion is that regardless of the model or parameters used, compositions can be found for the proto-Earth and impactor mantles that reproduce the compositions of the present-day terrestrial and lunar mantles. Thus, the Hf/W ratios and ε^{182}W values of the terrestrial and lunar mantles are not diagnostic of a particular formation scenario for the Moon. We can nevertheless evaluate if the canonical scenario of lunar formation by impact of a Mars-sized embryo with the proto-Earth is realistic by comparing the calculated compositions of the impactor and proto-Earth with those expected for an embryo and a planet. A characteristic feature that distinguishes planetary embryos from planets is their age [2,3]. Indeed, embryos are thought to have formed rapidly by runaway and oligarchic accretion of planetesimals and their formation age should be of the order of 10 Myr or less [125,138]. Planets on the other hand formed by collisions with embryos over a more protracted accretion history and their ages should be several tens of millions of years [113,114,131].

The inversion approach allows us to calculate the Hf/W (f) and ^{182}W/^{183}W (εW) values of the proto-Earth and impactor mantle. These values are sufficient to calculate a two-stage model age assuming that the bodies evolved with chondritic composition until the time when the core formed, assumed to be instantaneous [113]. These model ages are known to be inadequate to describe the accretion history of embryos and planets that differentiate as they grow. Yet, they provide a chronological framework to evaluate whether the calculated proto-Earth and impactor compositions are realistic. Regardless of the uncertainties in the model parameters, the two-stage model ages for the impactor range between approximately 10 and 20 Myr while the proto-Earth

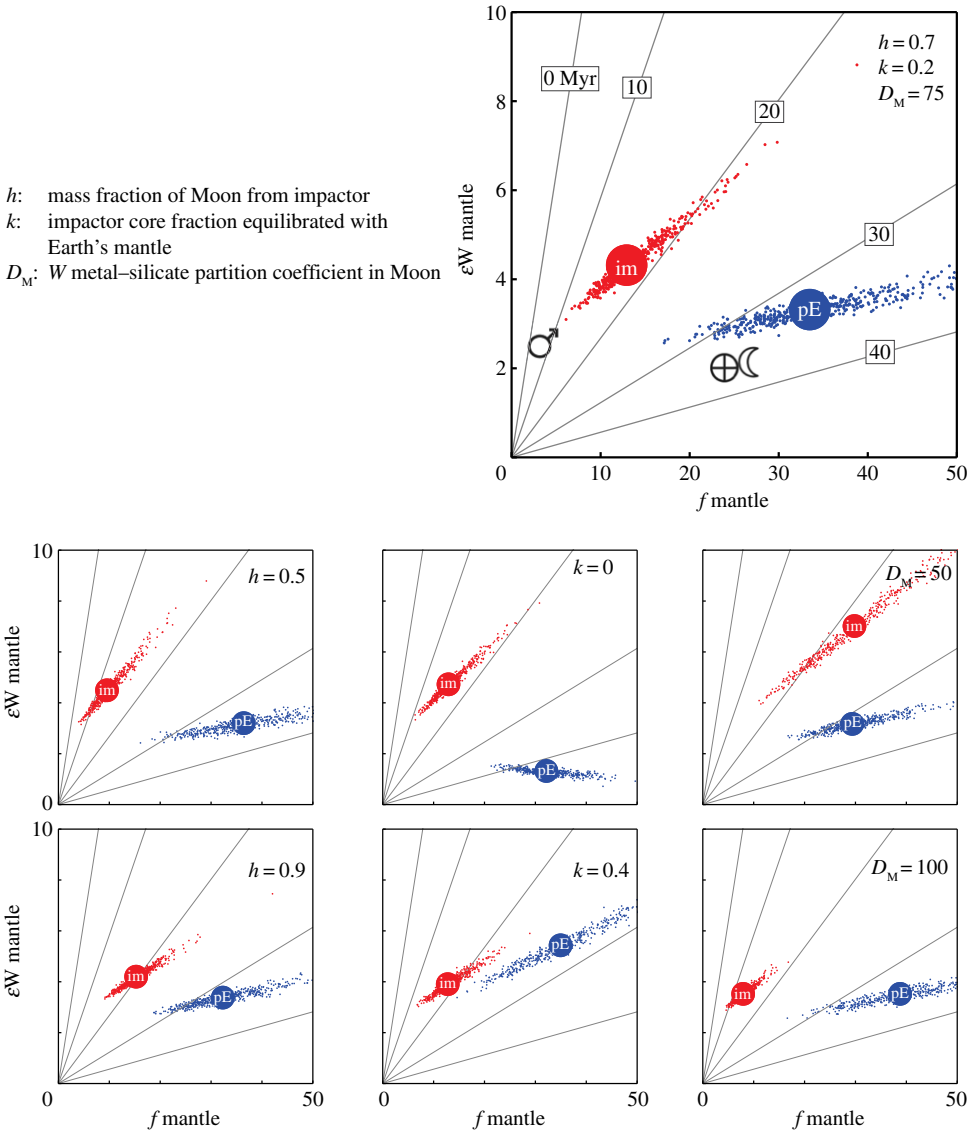

Figure 6. Tungsten isotopic compositions (εW) and Hf/W ratios (f) of the Moon-forming impactor (im, red symbols) and proto-Earth (pE, blue symbols) mantles obtained by mass-balance including 500 Monte Carlo simulations of the input parameter uncertainties (the governing equations are provided as the electronic supplementary material; see equations (23), (25), (39) and (41)). Values of terrestrial, lunar and Martian mantles are shown for comparison. The model parameters correspond to canonical models of the formation of the Moon and are compiled in table 1. The parameters that are allowed to vary in the different panels are the ones that affect the results the most: the degree of metal–silicate equilibration in the Earth's mantle after the giant impact ($0 < k < 0.4$), the metal–silicate partition coefficient of tungsten during lunar core formation ($50 < D_M < 100$), and the fraction of impactor material in the Moon ($0.5 < h < 0.9$). The lines correspond to two-stage model ages of core formation (i.e. times after Solar System formation when the cores of the impactor and proto-Earth would have formed in undifferentiated bodies of chondritic compositions). The εW values and Hf/W ratios of the lunar and terrestrial mantles can be explained in the framework of canonical models of the formation of the Moon by collision between an early formed embryo (two-stage model age of 10–20 Myr) and a proto-Earth that formed over a more protracted accretion history (two-stage model age of 30–40 Myr). (Online version in colour.)

Table 1. List of parameters and values used in Hf–W mass-balance. Derivation of the mass-balance can be found in the electronic supplementary material.

notation	meaning	value	reference/comment
μ	mass fraction late veneer Earth	0.0033	[127]
ν	mass fraction late veneer Moon	0.00023	[127]
γ	mass fraction mantle	0.68	assumed the same for impactor and proto-Earth
k	mass fraction of impactor core equilibrating with Earth's mantle	0–0.4	[134,135]; poorly constrained
g	mass fraction of Earth from impactor	0.11	Mars-sized impactor
D_E	$W_{metal-silicate}$ partition coefficient in Earth	54	calculated using $\gamma f_{BSE}/(1-\gamma)$
D_M	$W_{metal-silicate}$ partition coefficient in Moon	50–100	[128,136]
h	mass fraction of Moon from impactor	0.5–0.9	[9,137]
p	mass fraction of impactor mantle in Moon-forming impactor material	0.95–0.97	calculated using mass fraction lunar core $= (1-\nu)h(1-p)$
	mass fraction lunar core	0.025	[128,129]
$(Hf/W)_{BSE}$	Hf/W in BSE	27.4 ± 4.2	re-evaluation of [120–124] using chondritic Th/W and U/W of [125]
$(Hf/W)_{BSM}$	Hf/W in BSM	27.8 ± 3.3	re-evaluation of [120–124] using chondritic Th/W and U/W of [125]
$(Hf/W)_{CHUR}$	Hf/W in chondrites	1.04 ± 0.13	[117]
εW_{BSE}	$^{182}W/^{183}W$ of BSE relative to CHUR	1.9 ± 0.1	[117]
εW_{BSM}	$^{182}W/^{183}W$ of BSM relative to CHUR	2.1 ± 0.1	[19]

model ages range between approximately 20 and 40 Myr (figure 6). These accretion time scales are very realistic as Mars, which may be a stranded planetary embryo, has a two-stage model age of approximately 6 Myr [2] and the Earth, a fully-grown terrestrial planet, has a two-stage model age of approximately 35 Myr [114] (figure 6). The compositions of the impactor and proto-Earth are also well within the range of values predicted by n-body simulations [132].

The inversion approach shows that the Hf/W and $^{182}W/^{183}W$ ratios of the Earth and Moon can be readily explained in the framework of a canonical model of the giant impact involving collision between a Mars-sized early formed embryo with a proto-Earth that experienced a more protracted accretion history. The fact that the lunar composition resembles the terrestrial composition remains puzzling but it may just be a coincidence and we note that the Hf/W and $\varepsilon^{182}W$ values of the Moon are still very uncertain and more recent measurements have revealed a significant difference in $\varepsilon^{182}W$ values between the lunar and terrestrial mantles [19].

5. Differences and similarities in chemical compositions

The chemical compositions of lunar rocks show similarities and differences with their terrestrial equivalent, which can provide important constraints on models of the formation of the Moon. For example, the lunar mantle composition may plot off the trend defined by other planetary bodies in the diagram of δ^{30}Si versus Mg/Si (figure 5), questioning the idea that the Moon inherited its δ^{30}Si value from the proto-Earth mantle after removal of silicon into the terrestrial core. The Mg/Si ratio of the lunar mantle reflects the ratio of pyroxene (Mg/Si $\approx$ 1) to olivine (Mg/Si $\approx$ 2), which is uncertain. As a result, it is impossible to tell for sure if the Mg/Si ratio of the Moon is like chondrites or the silicate Earth. Other aspects of the lunar composition relevant to its origin and its relationship to Earth are discussed below.

The lunar Nb/Ta ratio has proved useful to quantify the contributions of the proto-Earth and impactor to the Moon. At high pressure, Nb becomes mildly siderophile, and thus may have partly sequestered into the Earth's core [139]. As a result, the Nb/Ta ratio in the silicate Earth is lower than that measured in chondrites. If the Moon was made predominantly of terrestrial mantle (with fractionated Nb/Ta ratio) and impactor material (with chondritic Nb/Ta ratio), then the lunar mantle should have a Nb/Ta ratio intermediate between chondrites and the silicate Earth and its value can constrain the proportions of each [140]. Münker *et al.* [124,140] have used the isotope dilution method to acquire a set of high-precision data for the seldom-determined refractory lithophile element Nb, along with its geochemical kindred Ta, Zr and Hf, in 22 lunar rocks (including two pyroclastic glass samples and one regolith breccia) and three lunar soils; and also in a variety of chondrites (figure 7). Based on a correlation between Zr/Hf and Nb/Ta, these authors infer that the bulk-Moon Nb/Ta (weight ratio) is 17.0 ± 0.8, significantly lower than the chondritic ratio (which they infer to be 19.9 ± 0.6), yet higher than the Nb/Ta of the BSE, which Münker *et al.* [140] inferred to be 14.0 ± 0.3. Münker's Nb/Ta inferences are consistent with the Moon being a giant impact mix of proto-Earth and impactor, in nearly equal proportion. Pfänder *et al.* [151] have admitted that the terrestrial Nb/Ta story is more complicated, and that 'up to approximately 30%' of the apparent depletion in Nb may actually be present in a high-Nb/Ta reservoir in the continental lithospheric mantle; i.e. that the BSE Nb/Ta may need to be corrected from 14.0 ± 0.3 to approximately 15.8. Nebel *et al.* [152] argue for yet another high-Nb/Ta reservoir, in the D″ layer, which they claim 'can readily explain the terrestrial Nb deficit, without the need to invoke core Nb storage'. They conjecture that this layer formed by sinking of an urKREEP analogue at the end of terrestrial magma ocean solidification. However, as this probably did not happen before the formation of the Moon, this scenario provides no viable mechanism to explain the Nb/Ta depletion relative to chondrites in the bulk Moon.

The Moon's component of non-core iron (FeO) is roughly a factor of 1.3 higher than the Earth's (7.7 wt% FeO in its 0.68 weight-fraction mantle; literature consensus reviewed in [153]). Yet, the Moon's small core [129] adds only 1–2 wt% to its total iron content, which is thus lower by a factor of 3–4 compared with the Earth's total iron content of approximately 34 wt% (of which 28 wt% is core Fe).

Recent measurements of lunar rocks have revealed that 'water' (OH) is vastly more abundant in the Moon than previously thought [154–158]. Still, the Moon is clearly depleted in volatile components and water may be heterogeneously distributed in the lunar interior, with most of it being dry [159,160]. Lunar rocks show depletion relative to their terrestrial counterparts by a factor of 5–10 in the major volatile element Na, and by factors of roughly 20 for volatile trace elements such as In and Bi [161]. The well-constrained ratio K/Th (the two elements behave similarly during melting and crystallization, even though K is volatile and Th is a refractory) is lower in lunar rocks than in terrestrial rocks by a factor of about 5 [162].

It is often suggested that the Moon is enriched, compared to the BSE, in the whole class of refractory lithophile elements (the major oxides Al_2O_3 and CaO, the minor TiO_2 and about 25 trace elements, including heat-producing U and Th, and the rare earth elements) [162,163]. However, depletions in volatile elements do not necessarily imply significant enrichments in refractory elements. Total depletion of every constituent with cosmochemical volatility (solar

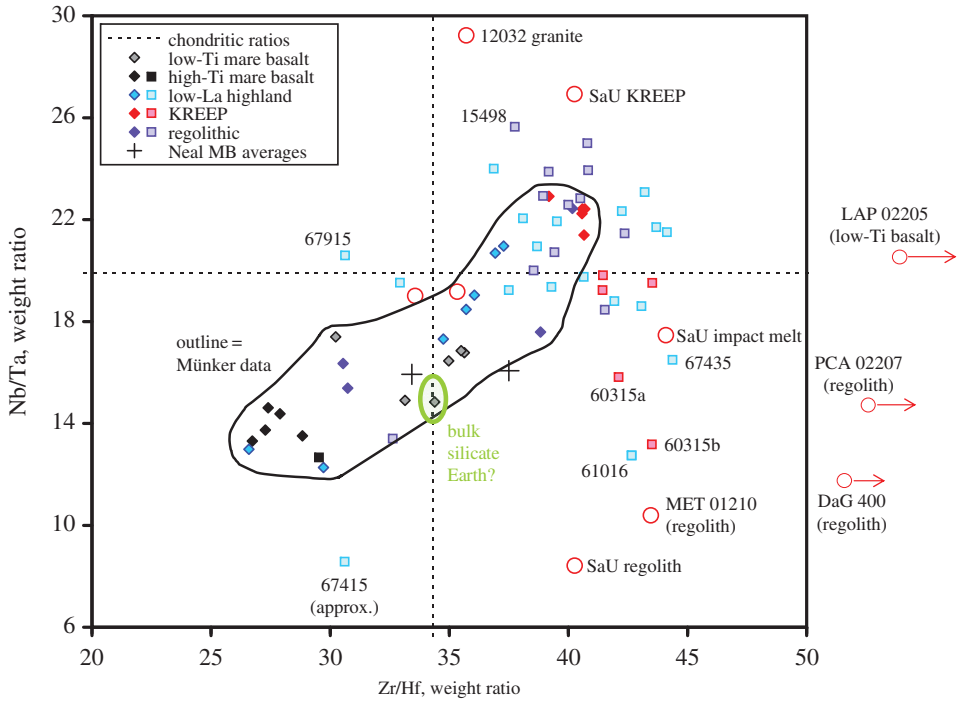

Figure 7. Plot of Zr/Hf versus Nb/Ta for lunar materials. Diamond symbols and chondritic ratios are from isotope dilution [124]. Other data show great scatter in comparison to the trend of Münker [124]. Square symbols are from instrumental neutron activation analysis by the Mainz laboratory ([141] and several Wänke *et al.* papers cited therein, e.g. [142]). Open circle symbols are from other, more recent literature [143–149]. Two cross symbols indicate averages for low-Ti and high-Ti mare basalts (with Zr/Hf = 37.5 and 33.4, respectively) from the large dataset of inductively coupled plasma mass spectrometry analyses by Neal [150]. Neal's data show more scatter and also systematic bias, mainly towards higher Zr/Hf, in comparison to Münker's [124] mare basalt data. Otherwise, in no case are separately obtained analyses averaged for purposes of this diagram. However, the datum for Nb in the tiny 12 032 granite rocklet [149] is based on a modal recombination technique whose accuracy and precision are hard to estimate. The vertical oval 'BSE' indicates by its Nb/Ta range the composition estimated by Münker *et al.* [140] and the modification envisaged by Pfänder *et al.* [151], i.e. 14 and 'up to' 15.8, respectively. The true uncertainty in this composition is difficult to assess. The lunar 'regolithic' category includes both soils and regolith breccias. For simplicity, all non-regolithic highland rocks are divided into just two categories: 'low-La' and KREEP, distinguished on the basis of the light rare earth element La (analysed 'low-La' rocks have La $< 40\ \mu g\ g^{-1}$; KREEP rocks have 50–113 $\mu g\ g^{-1}$). For the three recent literature (open circle) points plotted beyond the right edge of the diagram, actual reported Zr/Hf ratios are 58, 70 and 84, for DaG 400, PCA 02207 and LAP 02205, respectively [146,148]. (Online version in colour.)

nebula condensation temperature [164]) between those of SiO_2 and H_2O from even the most volatile-rich (CI) type of chondrite would increase the concentrations of all elements more refractory than Si by a factor of only 1.22. For 10 other types of chondrites, the increase would be merely a factor of 1.02–1.09 [165]. The motivation for the refractory-enrichment hypothesis has plummeted in recent years. Orbital γ-ray spectroscopy revealed that the central nearside region of the Apollo landing sites is atypically thorium-rich [166,167] and refined analyses of the limited lunar seismological dataset indicated that the crust, which presumably contains a major fraction of the Moon's total refractory lithophiles, is much thinner than previously supposed [168,169]. Most recently, gravity results from the GRAIL mission confirmed (or even strengthened) the thin crust models, and also revealed that the crust is far more porous (less dense) than previously supposed [170]. The mass of the lunar crust now appears lower by a factor of 2.4 in comparison to the premise of, for example, Taylor [162]. By substituting the crustal mass by Wieczorek *et al.* [170] for the one assumed by Warren [153], we derive an estimate of 65 ng g^{-1} for the bulk-Moon

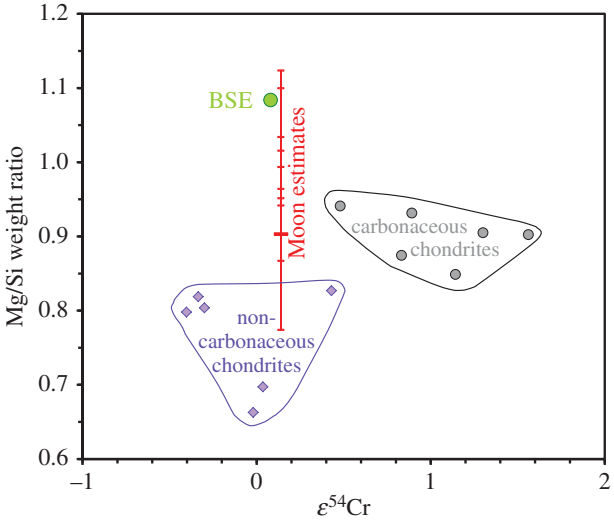

Figure 8. Compared to the non-carbonaceous types of chondrites that most closely match the Earth and Moon in isotope space (ε^{54}Cr is shown here as an example), both bodies have elevated MgO/SiO_2. The chondrite compositions are from [165]; ε^{54}Cr data are from sources compiled in [56] and the bulk-Moon composition estimates are from Warren [153] and earlier sources cited therein, plus Khan *et al.* [171]. The one lunar estimate with low MgO/SiO_2 is from [172]. Our new estimate (or assumption, $MgO/SiO_2 = 0.70$) is shown by the extra-large '—' symbol. (Online version in colour.)

Th content; and we model the other refractory lithophile elements in chondritic proportion to Th. These results show no significant difference in comparison to the consensus-estimated composition of the BSE (as reviewed in [153]). Wieczorek *et al.* [170] had also concluded that the Al_2O_3 content of the Moon was compatible with the terrestrial value.

The bulk Moon's most abundant oxide constituent, SiO_2, is not especially well constrained. It is customary to assume a similar SiO_2 concentration as in the BSE; in other words, one that results in a low-pressure *py* ($\equiv$ pyroxene/[pyroxene + olivine]) ratio of about 30 vol%. The *py* ratio is basically a function of MgO/SiO_2. Compared to the chondrite groups that provide the closest match in isotope space (figure 8 shows ε^{54}Cr as an example, see §2 for details), the Earth and the Moon have elevated MgO/SiO_2 in most estimates.

Another potentially important aspect of the Moon's bulk composition is the possibility that it features a considerable enrichment in FeO relative to the non-core Earth (7.7 wt%). The FeO content is in many respects most easily gauged by constraining the *mg* number, i.e. MgO/[MgO + FeO]. Certainly, the mare basalts, which typically have *mg* of about 40–60 mol% [161], derived from source regions with roughly 20 mol% lower *mg* than the Earth's mantle (89 mol%). Typical bulk-Moon *mg* estimates are in the range 81–84 mol%. However, the mare sources are believed to have formed mainly as cumulates from an evolved, late-stage remnant of the primordial magma ocean; and diminution of *mg* is one of the hallmarks of basaltic (and especially low-fO_2 basaltic) fractional crystallization. Also, melting of these sources was not aided by plate-tectonic vagaries, such as upwelling at mid-ocean ridges, so the most evolved parcels of the lunar mantle were probably favoured sites for anatexis. Warren [153,173] argued that the high *mg* of many Mg-suite highland rocks, and the moderate *mg* (up to 73 mol%) of highland regolith samples (blends of regional bulk upper crust), are indications that the lunar mantle as a whole is far less ferroan than the mare sources.

One way to constrain the bulk-Moon *mg* is by application of the improved array of geophysical constraints on the lunar interior. Unfortunately, no new seismic data have been acquired since 1977. The usual interpretation of the sparse seismic data pertinent to the deep mantle favours a low *mg* (e.g. [169,171,174]). A more Earth-like *mg* is possible, if the mantle's *py* ratio (otherwise not

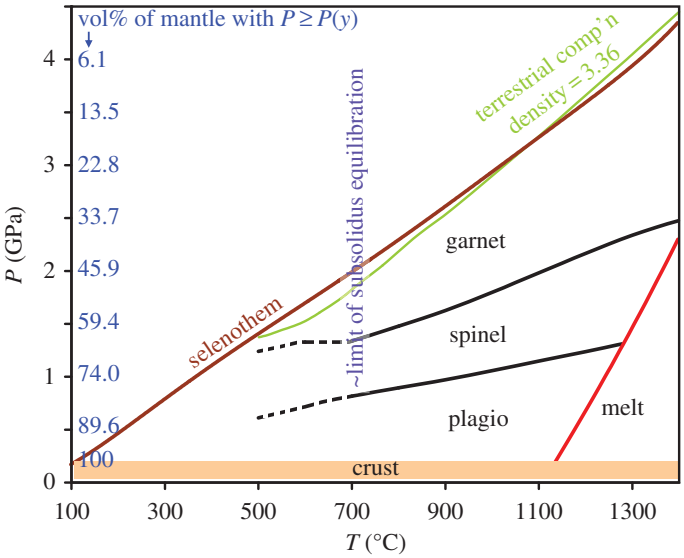

Figure 9. Plot of stability ranges of the various mantle Al-silicate phases as a function of temperature and pressure. The base diagram, from [177], is based on thermodynamical modelling for a terrestrial mantle composition. Similar results were obtained decades ago from experimental petrology [178]. At lunar fO_2, the range of spinel stability may be somewhat reduced, although that effect may be offset by the Moon's putatively lower *mg* [177]. The near-linear estimated lunar geotherm (selenotherm) [179] and the (terrestrial) mantle solidus [180] are also shown. After cooling for 4 Gyr to its present state, assuming equilibration was effective to approximately 700°C [181], approximately 65 vol% of the lunar mantle has garnet as the dominant Al-silicate, approximately 15 vol% has spinel and approximately 20 vol% has plagioclase. Assuming equilibration stalled at 800°C would alter these proportions to 60, 17 and 23 vol%, respectively. Also shown is a 3.36 g cm^{-3} iso-density contour from the modelling of [177]. The putatively lower *mg* of the lunar mantle should cause all such iso-density contours to shift, down and to the right, on this diagram. (Online version in colour.)

much constrained) is higher than Earth's [153]. The seismic data have been subjected to intense scrutiny to tease out constraints on the size and density of the lunar core. Weber *et al.* [129] (also see [174,175]) estimate the radius of the core to be 330 ± 20 km, and its mean density as 6.22 g cm^{-3}. The GRAIL mission has provided dramatically improved global gravity data [170], and as already discussed, the crust's average thickness is now inferred to be only approximately 34.5 km. Wieczorek *et al.* [170] cite 2.55 g cm^{-3} as their best estimate for the density of the 'highland crust'. Considering that a few vol% of the total crust is dense mare basalt, we assume 2.60 g cm^{-3} for the density for the total crust.

Together, these constraints on the masses and volumes of the Moon's crust and core, along with the Moon's radius of 1737.4 km and total lunar mass of 7.346×10^{22} kg [176], imply a precisely constrained density of 3.369 g cm^{-3} for the bulk mantle. Since the mantle consists preponderantly of just two similar-density mafic silicate minerals, olivine and pyroxene, this density constraint can be used to constrain the bulk-mantle *mg*. A few per cent of Al-silicate phase is also present, but in its current thermal condition most of the lunar interior has garnet as the preponderant Al-silicate (figure 9). In shallower parts, the mantle Al-silicate is spinel or plagioclase. The exact proportions will depend on the temperature to which the mantle mineralogy has equilibrated (after 4 Gyr of cooling) and the vertical distribution of Al within the mantle, but probably the overall mantle Al-silicate density is in the range 3.3–3.5 g cm^{-3}; i.e. so close to 3.369 g cm^{-3} that the assumed proportion of Al-silicate is inconsequential. We also assume, by implication from the bulk-Moon refractory lithophile inventory (see above) 0.25 vol% of ilmenite. Thermal expansion and pressure compression are modelled by the methods of Holland & Powell [182], but the mean temperature T_m of the lunar mantle is not well known. Models discussed by Nimmo *et al.* [179] and Kronrod & Kuskov [174] indicate 690–870°C; however older models reviewed in these

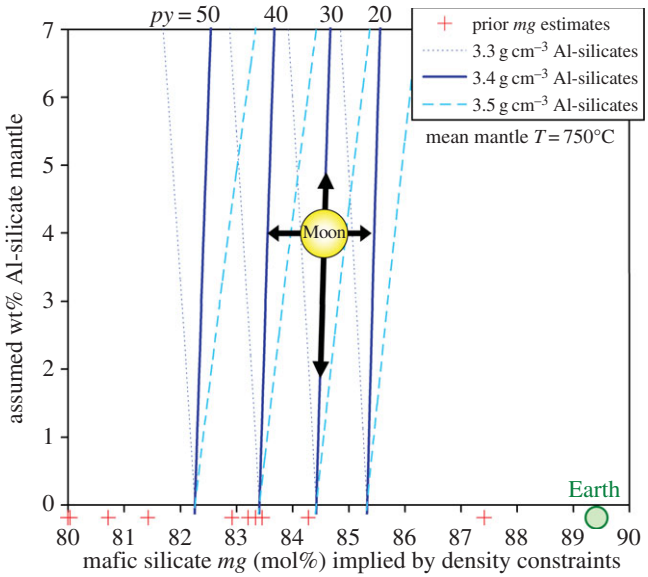

Figure 10. Plot of *mg* implied for the lunar bulk-mantle mafic silicate by density constraints. The *mg* is calculated to match an assumed bulk-mantle density of 3.369, as implied by constraints on volume and density of the crust from GRAIL [170], and the size and density of the core as estimated by Weber *et al.* [129]. Bulk-mantle mafic silicate *mg* implied by mixtures of pure olivine and pyroxene, along with 0.25 vol% of ilmenite, is shown at the bottom of the diagram (*py* is the ratio pyroxene/[pyroxene + olivine] in vol%). Curves that radiate upward from the bottom show potential effects of adding Al-silicate to the mix, with average density of the Al-silicates assumed to range from 3.3 to 3.5 g cm^{-3} (see text for discussion regarding this assumption, and regarding the likely amount of Al-silicate). The bulk-Moon *mg* is lower than the bulk lunar mantle mafic silicate *mg* plotted here, but only by 0.3–0.5 mol% (see text). Also shown for comparison are 10 previous estimates of the bulk-Moon *mg* ([153] and earlier sources cited therein, plus [171]). (Online version in colour.)

papers extend to both lower and (more commonly) higher extremes. Results for 750°C, shown in figure 10, suggest a bulk silicate Moon *mg* of 84.2 mol%. Results are shown as a function of T_m and *py* (and assuming 4 wt% of Al-silicate of mean density 3.4 g cm^{-3}) in figure 11. Note that the values plotted in the figures are inferences for the bulk-mantle mafic silicate *mg*. Translation into bulk silicate Moon *mg* requires a slight adjustment of minus approximately 0.4 mol% to compensate for the lower *mg* of the minor MgO + FeO stored in the crust, and in mantle spinel, garnet and ilmenite.

The biggest uncertainty in this approach is temperature. The Nimmo *et al.* [179] selenotherm implies (assuming *py* = 30 mol%) a bulk silicate Moon *mg* of 84.9 mol%; that of Kronrod & Kuskov [174] implies 82.9 mol%. The size of the core is another poorly known constraint. The nominal uncertainty in core radius cited by Weber *et al.* [129], 20 km, corresponds to precisely 1 mol% of implied bulk silicate Moon *mg* (a larger core implying higher *mg*). Although a lower *mg* is indicated if the *py* ratio is assumed high, there is a trade-off. The seismic constraints favour higher *mg* if *py* is increased [153]. Another caveat is that it is far from certain that the lunar mantle is devoid of the high-density phases that are normally assumed to be perfectly concentrated into the core. If the same 1 wt% concentration of Fe^0 that Frost *et al.* [183] (also see [184]) have proposed is stable (fails to sink into the core) in the deep terrestrial mantle were present in the lunar mantle where gravity is vastly lower, our *mg* results (figure 11) would need to be increased by 5 mol%.

Taking all of the above constraints (including the highland rock and regolith *mg* data) into consideration, our best estimate for the bulk silicate Moon *mg* is 85 mol%. This carries an implication that FeO is enriched by a factor of approximately 1.36 relative to the BSE. However, the uncertainty (one-sigma) in this estimate, realistically, is probably close to 0.2 (i.e. 2 mol% in *mg*); leaving a slight chance that the Moon's *mg* is as high as that of the BSE. Our estimate for the

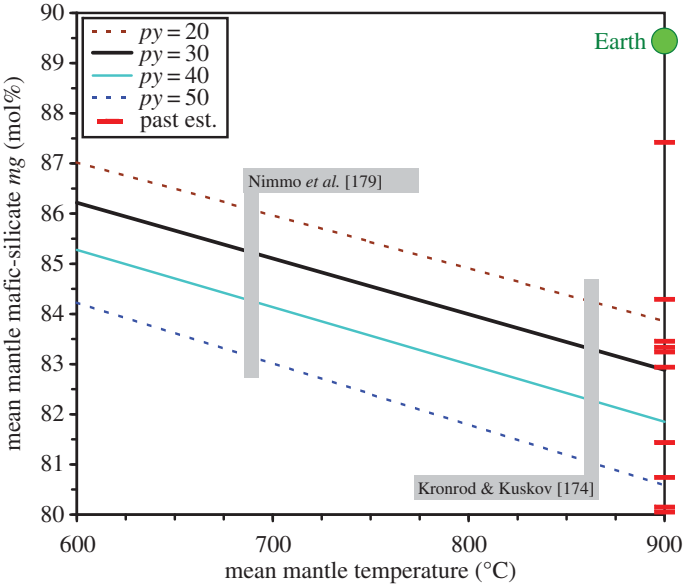

Figure 11. The *mg* implied for the lunar bulk-mantle mafic silicate by density constraints, plotted as a function of mantle temperature and *py* ratio (≡ pyroxene/(pyroxene + olivine) in vol%). The *mg* is calculated to match a bulk-mantle density of 3.369, as implied by constraints on volume and density of the crust from GRAIL [170], and the size and density of the core as estimated by Weber *et al.* [129]. Models assume the mantle is preponderantly olivine and pyroxene, along with 0.25 vol% of ilmenite and 4 wt% of Al-silicate. The exact proportion of Al-silicate is inconsequential, because the Al-silicates are preponderantly garnet, and thus are assumed to have average density of 3.4 g cm^{-3}, i.e. close to the bulk-mantle density (see text). The bulk-Moon *mg* is lower than the bulk lunar mantle mafic silicate *mg* plotted here, but only by 0.3–0.5 mol% (see text). Two recent estimates for the mean mantle temperature are shown [174,179]. Plotted at the right edge of the diagram are 10 previous estimates of the bulk-Moon *mg* ([153] and earlier sources cited therein, plus [171]). (Online version in colour.)

bulk composition of the bulk silicate Moon (table 2) is modified from the estimate of Warren [153] by the aforementioned increase in FeO (reducing *mg* from 87.4 to 85 mol%); by reduction of Th from 71 to 66 ng g^{-1}, with 27 other refractory lithophile elements, including Al and Ca, reduced by the same factor; and by moderation of the MgO/SiO_2 ratio from 1.1 × CI-chondritic to 1.0×. This MgO/SiO_2 modification keeps the $(MgO + FeO)/SiO_2$ ratio, and thus the implied *py* ratio, relatively unchanged.

6. Conclusion

All geochemical evidence pertaining to the question of the nature of material accreted by the Earth during its growth and after the completion of core formation is evaluated.

— Mixing models using CI, CM, CO + CV, O (ordinary) and E (enstatite) chondrites are evaluated using known ^{17}O, ^{48}Ca, ^{50}Ti, ^{54}Cr, ^{62}Ni and ^{92}Mo isotopic compositions as constraints [39]. The terrestrial signature for these isotopes can only be reproduced in models that have approximately 80–100% of enstatite chondrites in the mixture (figure 1). This illustrates the fact that the close similarity in isotopic composition between a fully grown planet like the Earth and a scoop of nebular dust represented by enstatite chondrites cannot be a mere coincidence but must reflect the fact that both formed from the same starting material and subsequently diverged in their chemical evolutions by nebular and disc processes. The inner disc was presumably quite uniform in its isotopic composition and most Earth-forming embryos were sourced from this reservoir, including the Moon-forming impactor.

Table 2. Estimated bulk composition of the non-core Moon, and for comparison some estimates from recent literature (nd, not determined).

	Th ng/g	Na_2O wt%	MgO wt%	Al_2O_3 wt%	SiO_2 wt%	CaO wt%	TiO_2 wt%	Cr_2O_3 wt%	MnO wt%	FeO wt%	Sc $\mu g\ g^{-1}$	V $\mu g\ g^{-1}$	Ga $\mu g\ g^{-1}$	La $\mu g\ g^{-1}$	U $\mu g\ g^{-1}$	sum wt%
new estimate (see text)	66	0.05	33.7	3.59	48.2	2.84	0.17	0.44	0.152	10.6	13.2	101	0.51	0.54	18	99.8
for comparison, three previous lunar bulk non-core composition models, and a consensus estimate for bulk composition of the non-core Earth																
Taylor [185]	114	0.09	32.0	6.0	43.4	4.5	0.30	0.61	0.15	13.0	19	150	nd	0.90	30	100.1
Warren [153]	nd	0.05	36.0	3.87	46.8	3.06	0.18	0.44	0.132	9.2	14.2	101	0.51	0.58	20	99.8
Khan *et al.* [171]	nd	nd	34	4.2	45.5	3.3	nd	nd	nd	12.2	nd	nd	nd	nd	nd	99.2
bulk non-core Earth[a]	75	0.34	36.4	3.97	47.2	3.19	0.19	0.40	0.132	7.67	15.2	92	3.7	0.58	20.0	99.5

[a] Average of seven estimates for bulk non-core Earth, from review by Warren [153].

— Molybdenum in the silicate Earth was delivered during the main stage of accretion, whereas ruthenium was delivered as part of the late veneer, after core formation. The silicate Earth Mo–Ru isotopic composition falls on the correlation defined by bulk meteorites [33,36,37] (figure 2). This indicates that the material accreted by the Earth before and after core formation did not change in its isotopic composition and was isotopically most similar to enstatite chondrites. This again supports constancy in the isotopic composition of the material accreted by the Earth, including the Moon-forming impactor.
— The isotopic composition of silicon in chondrites correlates with the Mg/Si ratio, reflecting nebular or disc fractionation. The BSE plots on the line defined by chondrites (figure 5). It is thus unknown to what extent the heavy silicon isotopic composition and high Mg/Si ratio of the silicate Earth relative to chondrites reflect partitioning of silicon in Earth's core or accretion from material already fractionated by nebular or disc processes. We argue that the similarity in the silicon isotope composition of the Moon and the silicate Earth reflects a similarity of nature between the Earth's building blocks and the Moon-forming impactor.
— A novel inversion approach allows us to calculate, for a given impact scenario, the Hf/W ratios and ε^{182}W values of the proto-Earth and impactor mantles from measured Hf/W ratios and ε^{182}W values of the present-day terrestrial and lunar mantles (figure 6). These compositions can then be used to calculate two-stage model ages of core formation. The similarity in tungsten isotopic composition (ε^{182}W) of the terrestrial and lunar mantles, which we take to be a coincidence (as is the similarity in ε^{182}W between the martian and terrestrial mantles), can be explained in the framework of canonical models of the formation of the Moon by collision between an early formed embryo (two-stage model age of 10–20 Myr) and the proto-Earth that formed over a more protracted accretion history (two-stage model age of 30–40 Myr).
— New results on the size of the lunar core and gravity data from the GRAIL mission allow us to refine the chemical composition of the Moon (table 2). Chemical similarities and differences exist between the Earth and Moon that are not well explained.

Overall, geochemical evidence suggests that the embryos accreted by the Earth were sourced from a region from the disc that had uniform isotopic composition most similar to enstatite chondrites, aubrites and ungrouped achondrite NWA 5363/5400. The similarity in isotopic composition between the Moon and the silicate Earth can be most naturally explained by the fact that the Moon-forming impactor originated from the same region of the disc as the other embryos that made the Earth. The ^{182}Hf–^{182}W characteristics of the Earth–Moon system are consistent with collision between an early formed embryo and a proto-Earth formed over a more protracted history. The canonical giant impact scenario remains a viable explanation of the origin of the Moon.

Acknowledgements. This contribution benefited from discussions with participants to the Origin of the Moon workshop at the Royal Society. We thank Alex Halliday and David Stevenson for making these interactions possible. Junjun Zhang, Andrew Davis, Alex Fedkin, Fatemeh Sedaghatpour, Franck Poitrasson, Francis Nimmo, Thorsten Kleine, Rich Walker, Mario Fischer-Gödde, François Tissot, Jim Chen, Dimitri Papanastassiou and Hiroshi Kobayashi are thanked for discussions. Insightful comments by Mathieu Touboul and an anonymous reviewer were greatly appreciated.

Funding statement. This work was supported by grants from NSF (EAR1144429 to N.D., EAR1056713 and EAR1340160 to F.Z.T.) and NASA (NNX12AH60G and NNX14AK09G to N.D., NNX13AH49G to P.W.).

References

1. Chambers JE, Wetherill GW. 1998 Making the terrestrial planets: n-body integrations of planetary embryos in three dimensions. *Icarus* **136**, 304–327. (doi:10.1006/icar.1998.6007)

2. Dauphas N, Chaussidon M. 2011 A perspective from extinct radionuclides on a young stellar object: the Sun and its accretion disk. *Annu. Rev. Earth Planet. Sci.* **39**, 351–386. (doi:10.1146/annurev-earth-040610-133428)
3. Morbidelli A, Lunine J, O'Brien D, Raymond S, Walsh K. 2012 Building terrestrial planets. *Annu. Rev. Earth Planet. Sci.* **40**, 251–275. (doi:10.1146/annurev-earth-042711-105319)
4. Hartmann WK, Davis DR. 1975 Satellite-sized planetesimals and lunar origin. *Icarus* **24**, 504–515. (doi:10.1016/0019-1035(75)90070-6)
5. Cameron AG, Ward WR. 1976 The origin of the Moon. In *7th Lunar and Planetary Science Conf. Abstracts*, p. 120.
6. Canup RM, Asphaug E. 2001 Origin of the Moon in a giant impact near the end of the Earth's formation. *Nature* **412**, 708–712. (doi:10.1038/35089010)
7. Ćuk M, Stewart ST. 2012 Making the Moon from a fast-spinning Earth: a giant impact followed by resonant despinning. *Science* **338**, 1047–1052. (doi:10.1126/science.1225542)
8. Canup RM. 2012 Forming a Moon with an Earth-like composition via a giant impact. *Science* **338**, 1052–1055. (doi:10.1126/science.1226073)
9. Reufer A, Meier MM, Benz W, Wieler R. 2012 A hit-and-run giant impact scenario. *Icarus* **221**, 296–299. (doi:10.1016/j.icarus.2012.07.021)
10. Clayton R, Mayeda T. 1975 Genetic relations between the Moon and meteorites. In *Proc. 6th Lunar and Planetary Science Conf.*, pp. 1761–1769.
11. Wiechert U, Halliday A, Lee D-C, Snyder G, Taylor L, Rumble D. 2001 Oxygen isotopes and the Moon-forming giant impact. *Science* **294**, 345–348. (doi:10.1126/science.1063037)
12. Spicuzza MJ, Day J, Taylor LA, Valley JW. 2007 Oxygen isotope constraints on the origin and differentiation of the Moon. *Earth Planet. Sci. Lett.* **253**, 254–265. (doi:10.1016/j.epsl.2006.10.030)
13. Hallis L, Anand M, Greenwood R, Miller MF, Franchi I, Russell S. 2010 The oxygen isotope composition, petrology and geochemistry of mare basalts: evidence for large-scale compositional variation in the lunar mantle. *Geochim. Cosmochim. Acta* **74**, 6885–6899. (doi:10.1016/j.gca.2010.09.023)
14. Zhang J, Dauphas N, Davis AM, Leya I, Fedkin A. 2012 The proto-Earth as a significant source of lunar material. *Nat. Geosci.* **5**, 251–255. (doi:10.1038/ngeo1429)
15. Qin L, Alexander CMD, Carlson RW, Horan MF, Yokoyama T. 2010 Contributors to chromium isotope variation of meteorites. *Geochim. Cosmochim. Acta* **74**, 1122–1145. (doi:10.1016/j.gca.2009.11.005)
16. Lugmair G, Shukolyukov A. 1998 Early Solar System timescales according to ^{53}Mn-^{53}Cr systematics. *Geochim. Cosmochim. Acta* **62**, 2863–2886. (doi:10.1016/S0016-7037(98)00189-6)
17. Herwartz D, Pack A, Friedrichs B, Bischoff A. 2014 Identification of the giant impactor Theia in lunar rocks. *Science* **344**, 1146–1150. (doi:10.1126/science.1251117)
18. Touboul M, Kleine T, Bourdon B, Palme H, Wieler R. 2007 Late formation and prolonged differentiation of the Moon inferred from W isotopes in lunar metals. *Nature* **450**, 1206–1209. (doi:10.1038/Nature06428)
19. Kleine T, Kruijer TS, Sprung P. 2014 Lunar ^{182}W and the age and origin of the Moon. In *45th Lunar and Planetary Science Conf.*, 2895.
20. Touboul M, Walker RJ, Puchtel IS. 2014 High-precision W isotope composition of the Moon for constraining late accretion and lunar formation. In *45th Lunar and Planetary Science Conf.*, 1851.
21. Armytage R, Georg R, Williams H, Halliday A. 2012 Silicon isotopes in lunar rocks: implications for the Moon's formation and the early history of the Earth. *Geochim. Cosmochim. Acta* **77**, 504–514. (doi:10.1016/j.gca.2011.10.032)
22. Fitoussi C, Bourdon B. 2012 Silicon isotope evidence against an enstatite chondrite Earth. *Science* **335**, 1477–1480. (doi:10.1126/science.1219509)
23. Zambardi T, Poitrasson F, Corgne A, Méheut M, Quitté G, Anand M. 2013 Silicon isotope variations in the inner Solar System: implications for planetary formation, differentiation and composition. *Geochim. Cosmochim. Acta* **121**, 67–83. (doi:10.1016/j.gca.2013.06.040)
24. Canup RM, Barr AC, Crawford DA. 2013 Lunar-forming impacts: high-resolution SPH and AMR-CTH simulations. *Icarus* **222**, 200–219. (doi:10.1016/j.icarus.2012.10.011)
25. Canup RM. 2004 Simulations of a late lunar-forming impact. *Icarus* **168**, 433–456. (doi:10.1016/j.icarus.2003.09.028)
26. Pahlevan K, Stevenson DJ. 2007 Equilibration in the aftermath of the lunar-forming giant impact. *Earth Planet. Sci. Lett.* **262**, 438–449 (doi:10.1016/j.epsl.2007.07.055)

27. Clayton RN, Grossman L, Mayeda TK. 1973 A component of primitive nuclear composition in carbonaceous meteorites. *Science* **182**, 485–488. (doi:10.1126/science.182.4111.485)
28. Clayton RN. 2002 Solar System: self-shielding in the solar nebula. *Nature* **415**, 860–861. (doi:10.1038/415860b)
29. Lyons J, Young E. 2005 CO self-shielding as the origin of oxygen isotope anomalies in the early solar nebula. *Nature* **435**, 317–320. (doi:10.1038/nature03557)
30. Yurimoto H, Kuramoto K. 2004 Molecular cloud origin for the oxygen isotope heterogeneity in the Solar System. *Science* **305**, 1763–1766. (doi:10.1126/science.1100989)
31. Dauphas N, Marty B, Reisberg L. 2002 Molybdenum evidence for inherited planetary scale isotope heterogeneity of the protosolar nebula. *Astrophys. J.* **565**, 640–644. (doi:10.1086/324597)
32. Dauphas N, Marty B, Reisberg L. 2002 Inference on terrestrial genesis from molybdenum isotope systematics. *Geophys. Res. Lett.* **29**, 1084. (doi:10.1029/2001gl014237)
33. Dauphas N, Davis AM, Marty B, Reisberg L. 2004 The cosmic molybdenum–ruthenium isotope correlation. *Earth Planet. Sci. Lett.* **226**, 465–475. (doi:10.1016/J.Epsl.2004.07.026)
34. Burkhardt C, Kleine T, Oberli F, Pack A, Bourdon B, Wieler R. 2011 Molybdenum isotope anomalies in meteorites: constraints on solar nebula evolution and origin of the Earth. *Earth Planet. Sci. Lett.* **312**, 390–400. (doi:10.1016/j.epsl.2011.10.010)
35. Chen J, Papanastassiou D, Wasserburg G. 2010 Ruthenium endemic isotope effects in chondrites and differentiated meteorites. *Geochim. Cosmochim. Acta* **74**, 3851–3862. (doi:10.1016/j.gca.2010.04.013)
36. Fischer-Gödde M, Burkhardt C, Kleine T. 2013 Origin of the late veneer inferred from Ru isotope systematics. In *44th Lunar and Planetary Science Conf.*, 2876.
37. Fischer-Gödde M, Kleine T, Burkhardt C, Dauphas N. 2014 Origin of nucleosynthetic isotope anomalies in bulk meteorites: evidence from coupled Ru and Mo isotopes in acid leachates of chondrites. In *45th Lunar and Planetary Science Conf.*, 2409.
38. Chen H-W, Lee T, Lee D-C, Jiun-San SJ, Chen J-C. 2011 ^{48}Ca heterogeneity in differentiated meteorites. *Astrophys. J. Lett.* **743**, L23. (doi:10.1088/2041-8205/743/1/L23)
39. Dauphas N, Chen JH, Zhang J, Papanastassiou DA, Davis AM, Travaglio C. Submitted. Calcium-48 isotopic anomalies in bulk chondrites and achondrites: evidence for a uniform isotopic reservoir in the inner protoplanetary disk.
40. Trinquier A, Elliott T, Ulfbeck D, Coath C, Krot AN, Bizzarro M. 2009 Origin of nucleosynthetic isotope heterogeneity in the solar protoplanetary disk. *Science* **324**, 374–376. (doi:10.1126/science.1168221)
41. Shukolyukov A, Lugmair G. 2006 Manganese–chromium isotope systematics of carbonaceous chondrites. *Earth Planet. Sci. Lett.* **250**, 200–213. (doi:10.1016/j.epsl.2006.07.036)
42. Trinquier A, Birck J-L, Allègre CJ. 2007 Widespread ^{54}Cr heterogeneity in the inner Solar System. *Astrophys. J.* **655**, 1179–1185. (doi:10.1086/510360)
43. Regelous M, Elliott T, Coath CD. 2008 Nickel isotope heterogeneity in the early Solar System. *Earth Planet. Sci. Lett.* **272**, 330–338. (doi:10.1016/j.epsl.2008.05.001)
44. Steele RC, Elliott T, Coath CD, Regelous M. 2011 Confirmation of mass-independent Ni isotopic variability in iron meteorites. *Geochim. Cosmochim. Acta* **75**, 7906–7925. (doi:10.1016/j.gca.2011.08.030)
45. Tang H, Dauphas N. 2012 Abundance, distribution, and origin of ^{60}Fe in the solar protoplanetary disk. *Earth Planet. Sci. Lett.* **359–360**, 248–263. (doi:10.1016/j.epsl.2012.10.011)
46. Qin L, Dauphas N, Wadhwa M, Markowski A, Gallino R, Janney PE, Bouman C. 2008 Tungsten nuclear anomalies in planetesimal cores. *Astrophys. J.* **674**, 1234–1241. (doi:10.1086/524882)
47. Andreasen R, Sharma M. 2007 Mixing and homogenization in the early Solar System: clues from Sr, Ba, Nd, and Sm isotopes in meteorites. *Astrophys. J.* **665**, 874–883. (doi:10.1086/518819)
48. Moynier F, Day JM, Okui W, Yokoyama T, Bouvier A, Walker RJ, Podosek FA. 2012 Planetary-scale strontium isotopic heterogeneity and the age of volatile depletion of early Solar System materials. *Astrophys. J.* **758**, 45. (doi:10.1088/0004-637X/758/1/45)
49. Hidaka H, Ohta Y, Yoneda S. 2003 Nucleosynthetic components of the early Solar System inferred from Ba isotopic compositions in carbonaceous chondrites. *Earth Planet. Sci. Lett.* **214**, 455–466. (doi:10.1016/S0012-821X(03)00393-5)

50. Carlson RW, Boyet M, Horan M. 2007 Chondrite barium, neodymium, and samarium isotopic heterogeneity and early earth differentiation. *Science* **316**, 1175–1178. (doi:10.1126/science.1140189)
51. Andreasen R, Sharma M. 2006 Solar nebula heterogeneity in p-process samarium and neodymium isotopes. *Science* **314**, 806–809. (doi:10.1126/science.1131708)
52. Dauphas N, Remusat L, Chen J, Roskosz M, Papanastassiou D, Stodolna J, Guan Y, Ma C, Eiler J. 2010 Neutron-rich chromium isotope anomalies in supernova nanoparticles. *Astrophys. J.* **720**, 1577–1591. (doi:10.1088/0004-637X/720/2/1577)
53. Qin L, Nittler LR, Alexander C, Wang J, Stadermann FJ, Carlson RW. 2011 Extreme ^{54}Cr-rich nano-oxides in the CI chondrite Orgueil—implication for a late supernova injection into the Solar System. *Geochim. Cosmochim. Acta* **75**, 629–644. (doi:10.1016/j.gca.2010.10.017)
54. Pahlevan K, Stevenson DJ, Eiler JM. 2011 Chemical fractionation in the silicate vapor atmosphere of the Earth. *Earth Planet. Sci. Lett.* **301**, 433–443. (doi:10.1016/j.epsl.2010.10.036)
55. Kokubo E, Ida S. 2000 Formation of protoplanets from planetesimals in the solar nebula. *Icarus* **143**, 15–27. (doi:10.1006/icar.1999.6237)
56. Warren PH. 2011 Stable-isotopic anomalies and the accretionary assemblage of the Earth and Mars: a subordinate role for carbonaceous chondrites. *Earth Planet. Sci. Lett.* **311**, 93–100. (doi:10.1016/j.epsl.2011.08.047)
57. Shukolyukov A, Lugmair G, Day J, Walker R, Rumble D, Nakashima D, Nagao K, Irving A. 2010 Constraints on the formation age, highly siderophile element budget and noble gas isotope compositions of Northwest Africa 5400: an ultramafic achondrite with terrestrial isotopic characteristics. In *41st Lunar and Planetary Science Conf. Abstracts*, p. 1492.
58. Javoy M. 1995 The integral enstatite chondrite model of the Earth. *Geophys. Res. Lett.* **22**, 2219–2222. (doi:10.1029/95GL02015)
59. Javoy M *et al.* 2010 The chemical composition of the Earth: enstatite chondrite models. *Earth Planet. Sci. Lett.* **293**, 259–268. (doi:10.1016/j.epsl.2010.02.033)
60. Kaminski E, Javoy M. 2013 A two-stage scenario for the formation of the Earth's mantle and core. *Earth Planet. Sci. Lett.* **365**, 97–107. (doi:10.1016/j.epsl.2013.01.025)
61. Savage PS, Moynier F. 2012 Silicon isotopic variation in enstatite meteorites: clues to their origin and Earth-forming material. *Earth Planet. Sci. Lett.* **361**, 487–496. (doi:10.1016/j.epsl.2012.11.016)
62. Chambers JE. 2001 Making more terrestrial planets. *Icarus* **152**, 205–224. (doi:10.1006/icar.2001.6639)
63. Fischer RA, Ciesla FJ. 2014 Dynamics of the terrestrial planets from a large number of N-body simulations. *Earth Planet. Sci. Lett.* **392**, 28–38. (doi:10.1016/j.epsl.2014.02.011)
64. Dauphas N, Morbidelli A. 2014 Geochemical and planetary dynamical views on the origin of Earth's atmosphere and oceans. In *Treatise on geochemistry*, 2nd edn, vol. 6 (eds HD Holland, KK Turekian), pp. 1–35. Oxford, UK: Elsevier.
65. Chou C-L. 1978 Fractionation of siderophile elements in the Earth's upper mantle. In *Proc. 9th Lunar and Planetary Science Conf.*, pp. 219–230.
66. Dauphas N, Marty B. 2002 Inference on the nature and the mass of Earth's late veneer from noble metals and gases. *J. Geophys. Res.* **107**, 5129. (doi:10.1029/2001JE001617)
67. Walker RJ. 2009 Highly siderophile elements in the Earth, Moon and Mars: update and implications for planetary accretion and differentiation. *Chem. Erde Geochem.* **69**, 101–125. (doi:10.1016/j.chemer.2008.10.001)
68. Wang Z, Becker H. 2013 Ratios of S, Se and Te in the silicate Earth require a volatile-rich late veneer. *Nature* **499**, 328–331. (doi:10.1038/nature12285)
69. Dauphas N. 2013 Geochemistry: sulphur from heaven and hell. *Nature* **501**, 175–176. (doi:10.1038/nature12554)
70. König S, Lorand J-P, Luguet A, Graham Pearson D. 2014 A non-primitive origin of near-chondritic S–Se–Te ratios in mantle peridotites; implications for the Earth's late accretionary history. *Earth Planet. Sci. Lett.* **385**, 110–121. (doi:10.1016/j.epsl.2013.10.036)
71. Magna T, Wiechert U, Halliday AN. 2006 New constraints on the lithium isotope compositions of the Moon and terrestrial planets. *Earth Planet. Sci. Lett.* **243**, 336–353. (doi:10.1016/j.epsl.2006.01.005)
72. Seitz H-M, Brey GP, Weyer S, Durali S, Ott U, Münker C, Mezger K. 2006 Lithium isotope compositions of Martian and lunar reservoirs. *Earth Planet. Sci. Lett.* **245**, 6–18. (doi:10.1016/j.epsl.2006.03.007)

73. Liu Y, Spicuzza MJ, Craddock PR, Day J, Valley JW, Dauphas N, Taylor LA. 2010 Oxygen and iron isotope constraints on near-surface fractionation effects and the composition of lunar mare basalt source regions. *Geochim. Cosmochim. Acta* **74**, 6249–6262. (doi:10.1016/j.gca.2010.08.008)
74. Sedaghatpour F, Teng F-Z, Liu Y, Sears DW, Taylor LA. 2013 Magnesium isotopic composition of the Moon. *Geochim. Cosmochim. Acta* **120**, 1–16. (doi:10.1016/j.gca.2013.06.026)
75. Sharp Z, Shearer C, McKeegan K, Barnes J, Wang Y. 2010 The chlorine isotope composition of the Moon and implications for an anhydrous mantle. *Science* **329**, 1050–1053. (doi:10.1126/science.1192606)
76. Humayun M, Clayton RN. 1995 Potassium isotope cosmochemistry: genetic implications of volatile element depletion. *Geochim. Cosmochim. Acta* **59**, 2131–2148. (doi:10.1016/0016-7037(95)00132-8)
77. Wiesli RA, Beard BL, Taylor LA, Johnson CM. 2003 Space weathering processes on airless bodies: Fe isotope fractionation in the lunar regolith. *Earth Planet. Sci. Lett.* **216**, 457–465. (doi:10.1016/S0012-821X(03)00552-1)
78. Poitrasson F, Halliday AN, Lee DC, Levasseur S, Teutsch N. 2004 Iron isotope differences between Earth, Moon, Mars and Vesta as possible records of contrasted accretion mechanisms. *Earth Planet. Sci. Lett.* **223**, 253–266. (doi:10.1016/J.Epsl.2004.04.032).
79. Weyer S, Anbar AD, Brey GP, Munker C, Mezger K, Woodland AB. 2005 Iron isotope fractionation during planetary differentiation. *Earth Planet. Sci. Lett.* **240**, 251–264. (doi:10.1016/J.Epsl.2005.09.023).
80. Paniello RC, Day JM, Moynier F. 2012 Zinc isotopic evidence for the origin of the Moon. *Nature* **490**, 376–379. (doi:10.1038/nature11507)
81. Seitz H-M, Brey GP, Lahaye Y, Durali S, Weyer S. 2004 Lithium isotopic signatures of peridotite xenoliths and isotopic fractionation at high temperature between olivine and pyroxenes. *Chem. Geol.* **212**, 163–177. (doi:10.1016/j.chemgeo.2004.08.009)
82. Jeffcoate A, Elliott T, Kasemann S, Ionov D, Cooper K, Brooker R. 2007 Li isotope fractionation in peridotites and mafic melts. *Geochim. Cosmochim. Acta* **71**, 202–218. (doi:10.1016/j.gca.2006.06.1611)
83. Eiler JM. 2001 Oxygen isotope variations of basaltic lavas and upper mantle rocks. *Rev. Mineral. Geochem.* **43**, 319–364. (doi:10.2138/gsrmg.43.1.319)
84. Teng F-Z, Li W-Y, Ke S, Marty B, Dauphas N, Huang S, Wu F-Y, Pourmand A. 2010 Magnesium isotopic composition of the Earth and chondrites. *Geochim. Cosmochim. Acta* **74**, 4150–4166. (doi:10.1016/j.gca.2010.04.019)
85. Fitoussi C, Bourdon B, Kleine T, Oberli F, Reynolds BC. 2009 Si isotope systematics of meteorites and terrestrial peridotites: implications for Mg/Si fractionation in the solar nebula and for Si in the Earth's core. *Earth Planet. Sci. Lett.* **287**, 77–85. (doi:10.1016/j.epsl.2009.07.038)
86. Armytage R, Georg R, Savage P, Williams H, Halliday A. 2011 Silicon isotopes in meteorites and planetary core formation. *Geochim. Cosmochim. Acta* **75**, 3662–3676. (doi:10.1016/j.gca.2011.03.044)
87. Savage P, Georg R, Armytage R, Williams H, Halliday A. 2010 Silicon isotope homogeneity in the mantle. *Earth Planet. Sci. Lett.* **295**, 139–146. (doi:10.1016/j.epsl.2010.03.035)
88. Savage PS, Georg RB, Williams HM, Burton KW, Halliday AN. 2011 Silicon isotope fractionation during magmatic differentiation. *Geochim. Cosmochim. Acta* **75**, 6124–6139. (doi:10.1016/j.gca.2011.07.043)
89. Sharp Z, Barnes J, Brearley A, Chaussidon M, Fischer T, Kamenetsky V. 2007 Chlorine isotope homogeneity of the mantle, crust and carbonaceous chondrites. *Nature* **446**, 1062–1065. (doi:10.1038/nature05748)
90. Bonifacie M, Jendrzejewski N, Agrinier P, Humler E, Coleman M, Javoy M. 2008 The chlorine isotope composition of Earth's mantle. *Science* **319**, 1518–1520. (doi:10.1126/science.1150988)
91. Humayun M, Clayton RN. 1995 Precise determination of the isotopic composition of potassium: application to terrestrial rocks and lunar soils. *Geochim. Cosmochim. Acta* **59**, 2115–2130. (doi:10.1016/0016-7037(95)00131-X)
92. Weyer S, Ionov DA. 2007 Partial melting and melt percolation in the mantle: the message from Fe isotopes. *Earth Planet. Sci. Lett.* **259**, 119–133. (doi:10.1016/J.Epsl.2007.04.033).
93. Craddock PR, Warren JM, Dauphas N. 2013 Abyssal peridotites reveal the near-chondritic Fe isotopic composition of the Earth. *Earth Planet. Sci. Lett.* **365**, 63–76. (doi:10.1016/j.epsl.2013.01.011)

94. Georg RB, Halliday AN, Schauble EA, Reynolds BC. 2007 Silicon in the Earth's core. *Nature* **447**, 1102–1106. (doi:10.1038/nature05927)
95. Chakrabarti R, Jacobsen SB. 2010 Silicon isotopes in the inner Solar System: implications for core formation, solar nebular processes and partial melting. *Geochim. Cosmochim. Acta* **74**, 6921–6933. (doi:10.1016/j.gca.2010.08.034)
96. Zambardi T, Poitrasson F. 2011 Precise determination of silicon isotopes in silicate rock reference materials by MC-ICP-MS. *Geostand. Geoanal. Res.* **35**, 89–99. (doi:10.1111/j.1751-908X.2010.00067.x)
97. Pringle EA, Savage PS, Badro J, Barrat J-A, Moynier F. 2013 Redox state during core formation on asteroid 4-Vesta. *Earth Planet. Sci. Lett.* **373**, 75–82. (doi:10.1016/j.epsl.2013.04.012)
98. Hin RC. 2012 Stable isotope behaviour during planetary differentiation. Dissertation, Eidgenössische Technische Hochschule ETH Zürich, no. 20825.
99. Badro J, Fiquet G, Guyot F, Gregoryanz E, Occelli F, Antonangeli D, d'Astuto M. 2007 Effect of light elements on the sound velocities in solid iron: implications for the composition of Earth's core. *Earth Planet. Sci. Lett.* **254**, 233–238. (doi:10.1016/j.epsl.2006.11.025)
100. Shahar A, Hillgren VJ, Young ED, Fei Y, Macris CA, Deng L. 2011 High-temperature Si isotope fractionation between iron metal and silicate. *Geochim. Cosmochim. Acta* **75**, 7688–7697. (doi:10.1016/j.gca.2011.09.038)
101. Hin RC, Fitoussi C, Schmidt MW, Bourdon B. 2014 Experimental determination of the Si isotope fractionation factor between liquid metal and liquid silicate. *Earth Planet. Sci. Lett.* **387**, 55–66. (doi:10.1016/j.epsl.2013.11.016)
102. Shahar A, Ziegler K, Young ED, Ricolleau A, Schauble EA, Fei Y. 2009 Experimentally determined Si isotope fractionation between silicate and Fe metal and implications for Earth's core formation. *Earth Planet. Sci. Lett.* **288**, 228–234. (doi:10.1016/j.epsl.2009.09.025)
103. Hirose K, Labrosse S, Hernlund J. 2013 Composition and state of the core. *Annu. Rev. Earth Planet. Sci.* **41**, 657–691. (doi:10.1146/annurev-earth-050212-124007)
104. Drake MJ, Righter K. 2002 Determining the composition of the Earth. *Nature* **416**, 39–44. (doi:10.1038/416039a)
105. Campbell IH, O'Neill HSC. 2012 Evidence against a chondritic Earth. *Nature* **483**, 553–558. (doi:10.1038/nature10901)
106. McDonough WF, Sun S-S. 1995 The composition of the Earth. *Chem. Geol.* **120**, 223–253. (doi:10.1016/0009-2541(94)00140-4)
107. Taylor GJ. In press. The bulk composition of Mars. *Chem. Erde*
108. Toplis MJ *et al.* 2013 Chondritic models of 4 Vesta: implications for geochemical and geophysical properties. *Meteorit. Planet. Sci.* **48**, 2300–2315. (doi:10.1111/maps.12195)
109. Lehner S, Petaev M, Zolotov MY, Buseck P. 2012 Formation of niningerite by silicate sulfidation in EH3 enstatite chondrites. *Geochim. Cosmochim. Acta.* **101**, 34–56. (doi:10.1016/j.gca.2012.10.003)
110. Dauphas N, Teng F-Z, Arndt NT. 2010 Magnesium and iron isotopes in 2.7 Ga Alexo komatiites: mantle signatures, no evidence for Soret diffusion, and identification of diffusive transport in zoned olivine. *Geochim. Cosmochim. Acta* **74**, 3274–3291. (doi:10.1016/j.gca.2010.02.031)
111. Handler MR, Baker JA, Schiller M, Bennett VC, Yaxley GM. 2009 Magnesium stable isotope composition of Earth's upper mantle. *Earth Planet. Sci. Lett.* **282**, 306–313. (doi:10.1016/j.epsl.2009.03.031)
112. Bourdon B, Tipper ET, Fitoussi C, Stracke A. 2010 Chondritic Mg isotope composition of the Earth. *Geochim. Cosmochim. Acta* **74**, 5069–5083. (doi:10.1016/j.gca.2010.06.008)
113. Jacobsen SB. 2005 The Hf-W isotopic system and the origin of the Earth and Moon. *Annu. Rev. Earth Planet. Sci.* **33**, 531–570. (doi:10.1146/annurev.earth.33.092203.122614)
114. Kleine T, Touboul M, Bourdon B, Nimmo F, Mezger K, Palme H, Jacobsen SB, Yin Q-Z, Halliday AN. 2009 Hf–W chronology of the accretion and early evolution of asteroids and terrestrial planets. *Geochim. Cosmochim. Acta* **73**, 5150–5188. (doi:10.1016/j.gca.2008.11.047)
115. Harper Jr CL, Jacobsen SB. 1996 Evidence for ^{182}Hf in the early Solar System and constraints on the timescale of terrestrial accretion and core formation. *Geochim. Cosmochim. Acta* **60**, 1131–1153. (doi:10.1016/0016-7037(96)00027-0)
116. Halliday A, Rehkämper M, Lee D-C, Yi W. 1996 Early evolution of the Earth and Moon: new constraints from Hf-W isotope geochemistry. *Earth Planet. Sci. Lett.* **142**, 75–89. (doi:10.1016/0012-821X(96)00096-9)

117. Kleine T, Mezger K, Münker C, Palme H, Bischoff A. 2004 ^{182}Hf–^{182}W isotope systematics of chondrites, eucrites, and martian meteorites: chronology of core formation and early mantle differentiation in Vesta and Mars. *Geochim. Cosmochim. Acta* **68**, 2935–2946. (doi:10.1016/j.gca.2004.01.009)
118. Lee D-C, Halliday AN, Leya I, Wieler R, Wiechert U. 2002 Cosmogenic tungsten and the origin and earliest differentiation of the Moon. *Earth Planet. Sci. Lett.* **198**, 267–274. (doi:10.1016/S0012-821X(02)00533-2)
119. Kleine T, Palme H, Mezger K, Halliday AN. 2005 Hf-W chronometry of lunar metals and the age and early differentiation of the Moon. *Science* **310**, 1671–1674. (doi:10.1126/science.1118842)
120. Newsom HE, Sims KW, Noll PD, Jaeger WL, Maehr SA, Beserra TB. 1996 The depletion of tungsten in the bulk silicate earth: constraints on core formation. *Geochim. Cosmochim. Acta* **60**, 1155–1169. (doi:10.1016/0016-7037(96)00029-4)
121. Palme H, Rammensee W. 1982 The significance of W in planetary differentiation processes: evidence from new data on eucrites. In *Proc. 12th Lunar and Planetary Science Conf.*, pp. 949–964.
122. Arevalo Jr R, McDonough WF. 2008 Tungsten geochemistry and implications for understanding the Earth's interior. *Earth Planet. Sci. Lett.* **272**, 656–665. (doi:10.1016/j.epsl.2008.05.031)
123. König S, Münker C, Hohl S, Paulick H, Barth A, Lagos M, Pfänder J, Büchl A. 2011 The Earth's tungsten budget during mantle melting and crust formation. *Geochim. Cosmochim. Acta* **75**, 2119–2136. (doi:10.1016/j.gca.2011.01.031)
124. Münker C. 2010 A high field strength element perspective on early lunar differentiation. *Geochim. Cosmochim. Acta* **74**, 7340–7361. (doi:10.1016/j.gca.2010.09.021)
125. Dauphas N, Pourmand A. 2011 Hf-W-Th evidence for rapid growth of Mars and its status as a planetary embryo. *Nature* **473**, 489–492. (doi:10.1038/nature10077)
126. Halliday AN. 2008 A young Moon-forming giant impact at 70–110 million years accompanied by late-stage mixing, core formation and degassing of the Earth. *Phil. Trans. R. Soc. A* **366**, 4163–4181. (doi:10.1098/rsta.2008.0209)
127. Bottke WF, Walker RJ, Day JM, Nesvorny D, Elkins-Tanton L. 2010 Stochastic late accretion to Earth, the Moon, and Mars. *Science* **330**, 1527–1530. (doi:10.1126/science.1196874)
128. Rai N, van Westrenen W. 2014 Lunar core formation: new constraints from metal–silicate partitioning of siderophile elements. *Earth Planet. Sci. Lett.* **388**, 343–352. (doi:10.1016/j.epsl.2013.12.001)
129. Weber RC, Lin P-Y, Garnero EJ, Williams Q, Lognonné P. 2011 Seismic detection of the lunar core. *Science* **331**, 309–312. (doi:10.1126/science.1199375)
130. Canup RM. 2004 Dynamics of lunar formation. *Annu. Rev. Astron. Astrophys.* **42**, 441–475. (doi:10.1146/annurev.astro.41.082201.113457)
131. Halliday AN. 2004 Mixing, volatile loss and compositional change during impact-driven accretion of the Earth. *Nature* **427**, 505–509. (doi:10.1038/nature02275)
132. Nimmo F, O'Brien D, Kleine T. 2010 Tungsten isotopic evolution during late-stage accretion: constraints on Earth–Moon equilibration. *Earth Planet. Sci. Lett.* **292**, 363–370. (doi:10.1016/j.epsl.2010.02.003)
133. Morishima R, Golabek GJ, Samuel H. 2013 N-body simulations of oligarchic growth of Mars: implications for Hf–W chronology. *Earth Planet. Sci. Lett.* **366**, 6–16. (doi:10.1016/j.epsl.2013.01.036)
134. Rudge JF, Kleine T, Bourdon B. 2010 Broad bounds on Earth's accretion and core formation constrained by geochemical models. *Nat. Geosci.* **3**, 439–443. (doi:10.1038/ngeo872)
135. Dahl TW, Stevenson DJ. 2010 Turbulent mixing of metal and silicate during planet accretion—and interpretation of the Hf–W chronometer. *Earth Planet. Sci. Lett.* **295**, 177–186. (doi:10.1016/j.epsl.2010.03.038)
136. Righter K. 2002 Does the Moon have a metallic core? Constraints from giant impact modeling and siderophile elements. *Icarus* **158**, 1–13. (doi:10.1006/icar.2002.6859)
137. Canup RM. 2008 Accretion of the Earth. *Phil. Trans. R. Soc. A* **366**, 4061–4075. (doi:10.1098/rsta.2008.0101)
138. Kobayashi H, Dauphas N. 2013 Small planetesimals in a massive disk formed Mars. *Icarus* **225**, 122–130. (doi:10.1016/j.icarus.2013.03.006)
139. Wade J, Wood B. 2001 The Earth's 'missing' niobium may be in the core. *Nature* **409**, 75–78. (doi:10.1038/35051064)

140. Münker C, Pfänder JA, Weyer S, Büchl A, Kleine T, Mezger K. 2003 Evolution of planetary cores and the Earth–Moon system from Nb/Ta systematics. *Science* **301**, 84–87. (doi:10.1126/science.1084662)
141. Palme H *et al.* 1978 New data on lunar samples and achondrites and a comparison of the least fractionated samples from the Earth, the Moon and the eucrite parent body. In *Proc. 9th Lunar and Planetary Science Conf.*, pp. 25–57.
142. Wänke H *et al.* 1975 New data on the chemistry of lunar samples: primary matter in the lunar highlands and the bulk composition of the moon. In *Proc. 6th Lunar and Planetary Science Conf.*, pp. 1313–1340.
143. Barrat J, Chaussidon M, Bohn M, Gillet P, Göpel C, Lesourd M. 2005 Lithium behavior during cooling of a dry basalt: an ion-microprobe study of the lunar meteorite Northwest Africa 479 (NWA 479). *Geochim. Cosmochim. Acta* **69**, 5597–5609. (doi:10.1016/j.gca.2005.06.032)
144. Neal C, Kramer G. 2003 The composition of KREEP: a detailed study of KREEP basalt 15386. In *44th Lunar and Planetary Science Conf. Abstracts*, p. 2023.
145. Gnos E *et al.* 2004 Pinpointing the source of a lunar meteorite: implications for the evolution of the Moon. *Science* **305**, 657–659. (doi:10.1126/science.1099397)
146. Joy KH, Crawford IA, Downes H, Russell SS, Kearsley AT. 2006 A petrological, mineralogical, and chemical analysis of the lunar mare basalt meteorite LaPaz Icefield 02205, 02224, and 02226. *Meteorit. Planet. Sci.* **41**, 1003–1025. (doi:10.1111/j.1945-5100.2006.tb00500.x)
147. Joy K, Crawford IA, Anand M, Greenwood R, Franchi I, Russell S. 2008 The petrology and geochemistry of Miller Range 05035: a new lunar gabbroic meteorite. *Geochim. Cosmochim. Acta* **72**, 3822–3844. (doi:10.1016/j.gca.2008.04.032)
148. Anand M, Taylor LA, Floss C, Neal CR, Terada K, Tanikawa S. 2006 Petrology and geochemistry of LaPaz Icefield 02205: a new unique low-Ti mare-basalt meteorite. *Geochim. Cosmochim. Acta* **70**, 246–264. (doi:10.1016/j.gca.2005.08.018)
149. Seddio SM, Jolliff BL, Korotev RL, Zeigler RA. 2013 Petrology and geochemistry of lunar granite 12032, 366–19 and implications for lunar granite petrogenesis. *Am. Mineral.* **98**, 1697–1713. (doi:10.2138/am.2013.4330)
150. Neal CR. 2001 Interior of the Moon: the presence of garnet in the primitive deep lunar mantle. *J. Geophys. Res.* **106**, 27 865–27 885. (doi:10.1029/2000JE001386)
151. Pfänder JA, Jung S, Münker C, Stracke A, Mezger K. 2012 A possible high Nb/Ta reservoir in the continental lithospheric mantle and consequences on the global Nb budget: evidence from continental basalts from Central Germany. *Geochim. Cosmochim. Acta* **77**, 232–251. (doi:10.1016/j.gca.2011.11.017)
152. Nebel O, Van Westrenen W, Vroon P, Wille M, Raith M. 2010 Deep mantle storage of the Earth's missing niobium in late-stage residual melts from a magma ocean. *Geochim. Cosmochim. Acta* **74**, 4392–4404. (doi:10.1016/j.gca.2010.04.061)
153. Warren PH. 2005 'New' lunar meteorites: implications for composition of the global lunar surface, lunar crust, and the bulk Moon. *Meteorit. Planet. Sci.* **40**, 477–506. (doi:10.1111/j.1945-5100.2005.tb00395.x)
154. Saal AE, Hauri EH, Cascio ML, Van Orman JA, Rutherford MC, Cooper RF. 2008 Volatile content of lunar volcanic glasses and the presence of water in the Moon's interior. *Nature* **454**, 192–195. (doi:10.1038/nature07047)
155. McCubbin FM, Steele A, Hauri EH, Nekvasil H, Yamashita S, Hemley RJ. 2010 Nominally hydrous magmatism on the Moon. *Proc. Natl Acad. Sci. USA* **107**, 11 223–11 228. (doi:10.1073/pnas.1006677107)
156. Boyce JW, Liu Y, Rossman GR, Guan Y, Eiler JM, Stolper EM, Taylor LA. 2010 Lunar apatite with terrestrial volatile abundances. *Nature* **466**, 466–469. (doi:10.1038/nature09274)
157. Greenwood JP, Itoh S, Sakamoto N, Warren P, Taylor L, Yurimoto H. 2011 Hydrogen isotope ratios in lunar rocks indicate delivery of cometary water to the Moon. *Nat. Geosci.* **4**, 79–82. (doi:10.1038/ngeo1050)
158. Hui H, Peslier AH, Zhang Y, Neal CR. 2013 Water in lunar anorthosites and evidence for a wet early Moon. *Nat. Geosci.* **6**, 177–180. (doi:10.1038/ngeo1735)
159. Albarede F, Albalat E, Lee CTA. In press. An intrinsic volatility scale relevant to the Earth and Moon and the status of water in the Moon. *Meteorit. Planet. Sci.* (doi:10.1111/maps.12331)
160. Robinson KL, Taylor GJ. 2014 Heterogeneous distribution of water in the Moon. *Nat. Geosci.* **7**, 401–408. (doi:10.1038/ngeo2173).
161. Warren PH, Taylor GJ. 2014 The Moon. In *Treatise on geochemistry* (eds HD Holland, KK Turekian), pp. 213–250. Amsterdam, The Netherlands: Elsevier.

162. Taylor SR. 1982 *Planetary science: a lunar perspective*. Houston, TX: Lunar and Planetary Institute.
163. Taylor SR, Taylor GJ, Taylor L. 2006 The moon: a Taylor perspective. *Geochim. Cosmochim. Acta* **70**, 5904–5918. (doi:10.1016/j.gca.2006.06.262)
164. Wasson JT. 1985 *Meteorites: their record of early solar-system history*. New York, NY: WH Freeman and Co.
165. Jarosewich E. 1990 Chemical analyses of meteorites: a compilation of stony and iron meteorite analyses. *Meteoritics* **25**, 323–337. (doi:10.1111/j.1945-5100.1990.tb00717.x)
166. Prettyman T, Hagerty J, Elphic R, Feldman W, Lawrence D, McKinney G, Vaniman D. 2006 Elemental composition of the lunar surface: analysis of gamma ray spectroscopy data from Lunar Prospector. *J. Geophys. Res. Planets* **111**, E12007. (doi:10.1029/2005JE002656)
167. Yamashita N *et al.* 2010 Uranium on the Moon: global distribution and U/Th ratio. *Geophys. Res. Lett.* **37**, L10201. (doi:10.1029/2010GL043061)
168. Lognonné P, Gagnepain-Beyneix J, Chenet H. 2003 A new seismic model of the Moon: implications for structure, thermal evolution and formation of the Moon. *Earth Planet. Sci. Lett.* **211**, 27–44. (doi:10.1016/S0012-821X(03)00172-9)
169. Khan A, Pommier A, Neumann G, Mosegaard K. 2013 The internal structure of the Moon: a geophysical perspective. *Tectonophysics* **609**, 331–332. (doi:10.1016/j.tecto.2013.02.024)
170. Wieczorek MA *et al.* 2013 The crust of the Moon as seen by GRAIL. *Science* **339**, 671–675. (doi:10.1126/science.1231530)
171. Khan A, Maclennan J, Taylor SR, Connolly J. 2006 Are the Earth and the Moon compositionally alike? Inferences on lunar composition and implications for lunar origin and evolution from geophysical modeling. *J. Geophys. Res. Planets* **111**, E05005. (doi:10.1029/2005JE002608)
172. Buck WR, Toksoz MN. 1980 The bulk composition of the Moon based on geophysical constraints. In *Proc. 11th Lunar and Planetary Science Conf.*, pp. 2043–2058.
173. Warren PH. 1986 The bulk-Moon MgO/FeO ratio: a highlands perspective. In *Origin of the Moon* (eds WK Hartmann, RJ Phillips, GJ Taylor), pp. 279–310. Houston, TX: Lunar and Planetary Institute.
174. Kronrod V, Kuskov O. 2011 Inversion of seismic and gravity data for the composition and core sizes of the Moon. *Izv. Phys. Solid Earth* **47**, 711–730. (doi:10.1134/S1069351311070044)
175. Garcia RF, Gagnepain-Beyneix J, Chevrot S, Lognonné P. 2011 Very preliminary reference Moon model. *Phys. Earth Planet. Inter.* **188**, 96–113. (doi:10.1016/j.pepi.2011.06.015)
176. Konopliv A. 2013 The JPL lunar gravity field to spherical harmonic degree 660 from the GRAIL primary mission. *J. Geophys. Res. Planets* **118**, 1415–1434. (doi:10.1002/jgre.20097)
177. Simon NS, Podladchikov YY. 2008 The effect of mantle composition on density in the extending lithosphere. *Earth Planet. Sci. Lett.* **272**, 148–157. (doi:10.1016/j.epsl.2008.04.027)
178. Ringwood AE. 1975 *Composition and petrology of the Earth's mantle*. New York, NY: McGraw-Hill.
179. Nimmo F, Faul U, Garnero E. 2012 Dissipation at tidal and seismic frequencies in a melt-free Moon. *J. Geophys. Res. Planets* **117**, E09005. (doi:10.1029/2012JE004160)
180. Hirschmann MM. 2000 Mantle solidus: experimental constraints and the effects of peridotite composition. *Geochem. Geophys. Geosyst.* **1**, 1042. (doi:10.1029/2000GC000070)
181. Warren PH, Haack H, Rasmussen KL. 1991 Megaregolith insulation and the duration of cooling to isotopic closure within differentiated asteroids and the Moon. *J. Geophys. Res. Solid Earth* **96**, 5909–5923. (doi:10.1029/90JB02333)
182. Holland T, Powell R. 1998 An internally consistent thermodynamic data set for phases of petrological interest. *J. Metamorphic Geol.* **16**, 309–343. (doi:10.1111/j.1525-1314.1998.00140.x)
183. Frost DJ, Liebske C, Langenhorst F, McCammon CA, Trønnes RG, Rubie DC. 2004 Experimental evidence for the existence of iron-rich metal in the Earth's lower mantle. *Nature* **428**, 409–412. (doi:10.1038/nature02413)
184. Rohrbach A, Ballhaus C, Ulmer P, Golla-Schindler U, Schönbohm D. 2011 Experimental evidence for a reduced metal-saturated upper mantle. *J. Petrol.* **52**, 717–731. (doi:10.1093/petrology/egq101)
185. Taylor SR. 1999 The Moon. In *Encyclopedia of the solar system* (eds PR Weissman, L-A McFadden, TV Johnson), pp. 247–275. San Diego, CA: Academic Press.